Spin diffusion in resolved solid-state NMR spectra

D. Suter and R. R. Ernst
Laboratorium für Physikalische Chemie, Eidgenössische Technische Hochschule Ziirich, CH-8092 Ziirich, Switzerland
(Received *20* May *1985;* revised manuscript received 22 August 1985)

Spectral spin diffusion in resolved solid-state NMR spectra is analyzed for various types of systems, including dipolar coupled spin-+ systems in the presence of extraneous spins, and systems of quadrupolar spins with and without an additional dipolar reservoir. Diffusion of Zeeman and quadrupolar order via single-quantum and double-quantum spin-diffusion mechanisms is considered. Special attention is paid to the frequency offset dependence of the spin-diffusion rate. The theoretical predictions are verified by spin-diffusion measurements using two-dimensional spectroscopy techniques for ^{13}C deuterium, and ^{14}N resonance in single crystals.

I. INTRODUCTION

The term spin diffusion has been introduced by Bloembergen[1] in order to describe the transport of spin order through a crystalline lattice in the presence of a spin temperature gradient caused by relaxation of nuclear spins by paramagnetic impurities. Such a process transports spin polarization between spatially separated equivalent spins and is called spatial spin diffusion, while an exchange of polarization between spins with different resonance frequencies may be considered as a diffusion process in frequency space leading to spectral spin diffusion. Both processes are results of the same basic interaction, the dipole-dipole couplings of nuclear spins, but their observation is different. Changes in the spatial distribution of spin polarization are detected indirectly by measuring deviations from exponentiality during the relaxation process, while spectral spin diffusion is observed directly as an exchange of magnetization between resolved resonance lines.

The diffusion of spin order is responsible for numerous phenomena which are of importance both for measurement techniques (for example, in Hartmann-Hahn cross polarization[2–4]) as well as for the understanding of relaxation phenomena.[5–11] Spin diffusion can be used to obtain information about spatial proximity in solids[12–17] in analogy to the nuclear Overhauser effect in liquids.[18–22]

Spin diffusion requires energy-conserving processes which transport order between different spins. As long as the involved transition frequencies are degenerate, flip-flop processes mediated by the dipolar interaction are energy conserving and the Zeeman order of individual spins is no longer a constant of motion. It participates in a collective process which leads to an oscillatory exchange of order between coupled spins. The process may be strongly damped by additional neighbor interactions.

The situation is different in the case of resolved or partially overlapping resonance lines where s in diffusion has also been experimentally verified.[10,11,1',23] The dipole-dipole interaction between the two spins which exchange polarization is in this case too weak to compensate for the change in the Zeeman energy of the system associated with the transfer of population between spins with different resonance frequencies. Therefore, energy conservation requires particular attention. Several mechanisms have been proposed in the past which satisfy the principle of energy conservation, either by the cooperation of extraneous spins[23] or by multiple-quantum spin flips.[24,25]

Spectral spin diffusion among resolved resonances has particular experimental appeal for tracing out the pathways of diffusion. It yields information on the spatial proximity of uniquely identified sites and provides an attractive tool to study the structure of solids. Such techniques are aimed not so much at the investigation of crystalline materials which can well be studied by diffraction methods (especially if single crystals are available), but rather to obtain information on amorphous and heterogeneous solids, such as glasses and heterogeneous polymers[8,14,16,17]

To exploit the full potential of spectral spin-diffusion measurements, two-dimensional (2D) spectroscopy is a prerequisite. It not only maximizes the content and flux of information, but also facilitates the measurements and makes them truly routine (although sometimes rather time consuming). Several examples of 2D spin-diffusion measurements have recently been published.[14–17,23,26]

The spectral separation of the different sites can be due to chemical shifts exceeding the dipolar linewidth, as in ^{13}C resonance or quadmpolar interactions which are normally strong enough to dominate the spectrum. In the past, deuterium and ^{14}N spin diffusion has been investigated.[10,11,23,25] In combination with multiple pulse scaling of dipolar interactions and magic angle sample spinning, spectral spin-diffusion measurements are feasible also for strongly coupled proton and fluorine systems.[17]

In this paper we present a theoretical analysis of spectral spin diffusion for resolved resonance lines. We discuss and compare the various remedies which nature might use to satisfy the law of energy conservation. We support the theoretical considerations by new experimental data. The experiments which are presented have all been performed on single crystals. This turned out to be indispensable for a quantitative test of the theoretical predictions.

II. KINETICS OF SPECTRAL DIFFUSION

A. Basic formalism

The transport of spin order between different types of spins is most appropriately described by a set of coupled rate equations for the expectation values of the relevant observables. The number of such observables may become large in complicated spin systems. We will see, however, that it is often sufficient to concentrate on a small number of operators to obtain transport equations for the observables of interest. The formulation, as well as the mathematical tools, are closely analogous to those used in the theory of relaxation, with the relevant part of the system coupled not to the molecular lattice motions but to a heat bath consisting of the dipolar spin interactions. The interaction between system and environment is described by a deterministic quantum-mechanical formulation. The irreversibility which characterizes the spin-diffusion process enters through a perturbation treatment and through the concentration on a small number of observables.

We will develop the formalism for the exchange of polarization between two spins S_1 and S_2, coupled to a large number of further spins which do not directly participate in the exchange process but supply the energy needed to transfer polarization between nonequivalent spins. The two S spins represent either an isolated spin pair or two classes of equivalent spins.

The Hamiltonian which governs the motion of the full system is written in the form

$$\mathcal{H}=\mathcal{H}_S+\mathcal{H}_{SE}+\mathcal{H}_E\,, \tag{1}$$

where $\mathcal{H}_S$ describes the motion of the two representative S spins, $\mathcal{H}_E$ comprises the interactions among the extraneous spins, and $\mathcal{H}_{SE}$ represents the coupling terms. The following commutation relations hold:

$$[\mathcal{H}_S,\mathcal{H}_E]=0,\quad [\mathcal{H}_S,\mathcal{H}_{SE}]\neq 0,\quad [\mathcal{H}_E,\mathcal{H}_{SE}]\neq 0\,. \tag{2}$$

To calculate the rate constants by time-dependent perturbation theory, we split the Hamiltonian into two parts,

$$\mathcal{H}=\mathcal{H}_0+\mathcal{H}_1\,, \tag{3}$$

with

$$\mathcal{H}_0=\mathcal{H}_S+\mathcal{H}_E,\quad \mathcal{H}_1=\mathcal{H}_{SE}\,, \tag{4}$$

and transform the Liouville-von Neumann equation (with $\hbar=1$),

$$\dot{\sigma}=-i[\mathcal{H},\sigma]\,, \tag{5}$$

as usual into the interaction frame with respect to $\mathcal{H}_0$, defined by

$$\sigma^T(t)=\exp(i\mathcal{H}_0 t)\sigma(t)\exp(-i\mathcal{H}_0 t)\,. \tag{6}$$

In this representation the equation of motion is

$$\dot{\sigma}^T(t)=-i[\mathcal{H}_1^T(t),\sigma^T(t)]\,. \tag{7}$$

An iteration of Eq. (7) leads to a power-series expansion with respect to $\mathcal{H}_1$:

$$\dot{\sigma}^T(t)=-i[\mathcal{H}_1^T(t),\sigma^T(0)] - \int_0^t d\tau\{\mathcal{H}_1^T(t),[\mathcal{H}_1^T(t-\tau),\sigma^T(0)]\}+\cdots\,. \tag{8}$$

We expand the traceless part of the density operator in terms of a set of operators $\{A_i\}$

$$\sigma^T(t)=\sum_i a_i(t)A_i\,, \tag{9}$$

which are assumed to be orthogonal,

$$\mathrm{Tr}\{A_i^\dagger A_j\}=\delta_{ij}\mathrm{Tr}\{A_i^2\}\,, \tag{10}$$

and obtain differential equations for the coefficients $a_k(t)$ by inserting Eq. (9) into Eq. (8), multiplying both sides with A_k, and taking the trace:

$$\mathrm{Tr}\{A_k^2\}\dot{a}_k(t)=-i\sum_i a_i(0)\mathrm{Tr}\{[\mathcal{H}_1^T(t),A_i]A_k\}+\sum_i a_i(0)\int_0^t \mathrm{Tr}\{[\mathcal{H}_1^T(t),A_k][\mathcal{H}_1^T(t-\tau),A_i]\}d\tau\,. \tag{11}$$

If the conditions for the application of perturbation theory are fulfilled, the integrand in Eq. (11) vanishes before the coefficients $a_k(t)$ have changed appreciably. We may therefore extend the integration limit to infinity. We may in addition extend the validity of the second-order expansion by replacing $a_i(0)$ by $a_i(t)$. The resulting system of equations can be written in the form

$$\dot{a}_k(t)=\sum_i W_{ki}a_i(t)\,, \tag{12}$$

where the rate constants W_{ki} are given by

$$W_{ki}=(\mathrm{Tr}\{A_k^2\})^{-1}[-i\,\mathrm{Tr}\{[\mathcal{H}_1^T(t),A_i]A_k\} + \int_0^\infty \mathrm{Tr}\{[\mathcal{H}_1^T(t),A_k][\mathcal{H}_1^T(t-\tau),A_i]\}d\tau\,. \tag{13}$$

This formula has been used in similar form by Provotorov[27] and Goldman (Ref. 28, Chap. 4). It differs from that of semiclassical relaxation theory (see, e.g., Ref. 29, Chap. 8) by the missing ensemble average. The coupling to the environment is not described as a stochastic process but as a deterministic and reversible time evolution. Equations (12) and (13) still represent a description of system and environment. The apparent irreversibility of the spin-diffusion process is introduced by the restriction of the operator set $\{A_i\}$ to the few relevant observables of the system and by setting $a_i(t)=0$ for all other values of i. This implies the assumption of infinite temperature for the disregarded degrees of freedom, irrespective of the transfer of order. The thermodynamic aspects of spin diffusion will be discussed more thoroughly in Sec. III.

In the following paragraphs we will apply the expressions, Eqs. (12) and (13), to the calculation of spectral spin-diffusion rates in several systems. We treat first the simple case of two inequivalent spins $S=\frac{1}{2}$ coupled to a large number of I spins and apply in the following sections the results to more complicated situations.

B. Spectral spin diffusion between two spins $S=\frac{1}{2}$ in the presence of abundant I spins

A system of two spins $S=\frac{1}{2}$, coupled to abundant I spins, which form a large dipolar reservoir, can be regarded as a prototype for more complicated cases to be considered later. The full Hamiltonian $\mathcal{H}$ takes the explicit form

$$\begin{aligned}
&\mathcal{H}=\mathcal{H}_S+\mathcal{H}_{SS}+\mathcal{H}_{SI}+\mathcal{H}_{II}\ ,\\
&\mathcal{H}_S=\Omega_1 S_{1z}+\Omega_2 S_{2z}\ ,\\
&\mathcal{H}_{SS}=d\,[2S_{1z}S_{2z}-\tfrac{1}{2}(S_1^+S_2^-+S_1^-S_2^+)]\ ,\\
&\mathcal{H}_{SI}=\sum_i b_{1i}^{SI}2S_{1z}I_{iz}+\sum_i b_{2i}^{SI}2S_{2z}I_{iz}\ ,\\
&\mathcal{H}_{II}=\sum_{\substack{i,j\\ i<j}} b_{ij}^{II}[2I_{iz}I_{jz}-\tfrac{1}{2}(I_i^+I_j^-+I_i^-I_j^+)]\ ,
\end{aligned}\tag{14}$$

with

$$b_{ij}^{xy}=\frac{\mu_0}{4\pi}\gamma_x\gamma_y\hbar r_{ij}^{-3}P_2(\cos\Theta_{ij})\ .$$

The Zeeman interaction of the I spins has been disregarded, since in the limit of identical chemical shifts, it commutes with the remainder of the Hamiltonian and has no effect on S-S spin diffusion.

The relevant observable operators for spin diffusion between S_1 and S_2 are S_{1z} and S_{2z}. Since the total polarization operator $S_{1z}+S_{2z}$ commutes with the Hamiltonian and only flip-flop processes are involved in spin diffusion, the total S spin polarization is a constant of motion. It is therefore sufficient to consider the time evolution of the difference polarization operator $\frac{1}{2}(S_{1z}-S_{2z})$. Accordingly, we rewrite the two terms $\mathcal{H}_S$ and $\mathcal{H}_{SI}$:

$$\begin{aligned}
&\mathcal{H}_S=\mathcal{H}_\Sigma+\mathcal{H}_\Delta\ ,\\
&\mathcal{H}_\Sigma=(\Omega_1+\Omega_2)\tfrac{1}{2}(S_{1z}+S_{2z})\ ,\\
&\mathcal{H}_\Delta=(\Omega_1-\Omega_2)\tfrac{1}{2}(S_{1z}-S_{2z})\ ,
\end{aligned}\tag{15}$$

and

$$\begin{aligned}
&\mathcal{H}_{SI}=\mathcal{H}_{SI\Sigma}+\mathcal{H}_{SI\Delta}\ ,\\
&\mathcal{H}_{SI\Sigma}=(b_{1i}^{SI}+b_{2i}^{SI})(S_{1z}+S_{2z})I_{iz}\ ,\\
&\mathcal{H}_{SI\Delta}=(b_{1i}^{SI}-b_{2i}^{SI})(S_{1z}-S_{2z})I_{iz}\ .
\end{aligned}$$

The two terms $\mathcal{H}_\Sigma$ and $d\,2S_{1z}S_{2z}$, which commute with the observable $\frac{1}{2}(S_{1z}-S_{2z})$ as well as with the remainder of the Hamiltonian, can be disregarded.

Although the term $\mathcal{H}_{SI\Sigma}$ does not commute with $\mathcal{H}_{II}$, it does not affect the observable $\frac{1}{2}(S_{1z}-S_{2z})=S_z^{(23)}$. This can be understood by formally separating the term $\mathcal{H}_{II}$ into two mutually commuting parts

$$\mathcal{H}_{II}=\mathbb{1}^{(14)}\cdot\mathcal{H}_{II}+\mathbb{1}^{(23)}\cdot\mathcal{H}_{II}\ ,\tag{16}$$

where $\mathbb{1}^{(14)}$ and $\mathbb{1}^{(23)}$ are unity operators of the subsystems spanned by the functions $|1\rangle=|\alpha\alpha\rangle, |4\rangle=|\beta\beta\rangle$ and $|2\rangle=|\alpha\beta\rangle, |3\rangle=|\beta\alpha\rangle$ of the two S spins, respectively (see Fig. 1). In terms of spin operators they can be expressed by

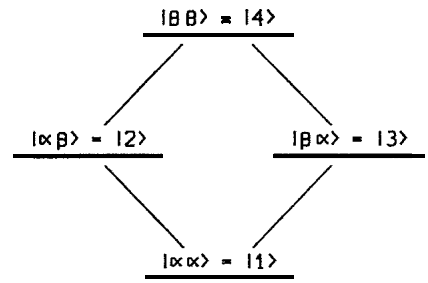

FIG. 1. Energy-level scheme for two spins $\frac{1}{2}$, indicating the numbering used in the text.

$$\mathbb{1}^{(14)}=\tfrac{1}{2}\mathbb{1}+2S_{1z}S_{2z},\quad \mathbb{1}^{(23)}=\tfrac{1}{2}\mathbb{1}-2S_{1z}S_{2z}\ .\tag{17}$$

The two parts of $\mathcal{H}_{II}$ act then either on the (1,4) or the (2,3) subsystem and are completely separated from each other.

We introduce further the single transition operators

$$\begin{aligned}
&S_x^{(23)}=\tfrac{1}{2}(S_1^+S_2^-+S_1^-S_2^+)\ ,\\
&S_y^{(23)}=-\tfrac{1}{2}i(S_1^+S_2^--S_1^-S_2^+)\ ,\\
&S_z^{(23)}=\tfrac{1}{2}(S_{1z}-S_{2z})\ ,
\end{aligned}\tag{18}$$

which fulfill the cyclic commutation relations of angular momentum operators, and rewrite the relevant part of the Hamiltonian as

$$\mathcal{H}^{(23)}=\delta S_z^{(23)}-dS_x^{(23)}+2\sum_i b_i S_z^{(23)}I_{iz}+\mathcal{H}_{II}^{(23)}\ ,\tag{19}$$

where

$$\delta=\Omega_1-\Omega_2,\quad b_i=b_{1i}^{SI}-b_{2i}^{SI}\ .\tag{20}$$

Only terms relevant for the (2,3) subsystem have been kept. They correspond to the upper row of boxes in Fig. 2. Equation (19) shows that the problem of spin diffusion

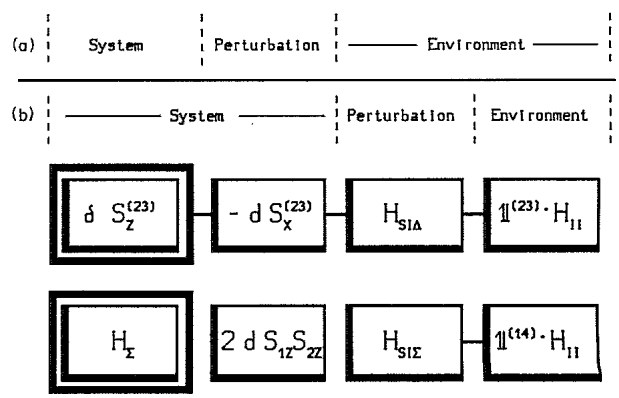

FIG. 2. Commutation diagram for two dipolar coupled S spins in the presence of abundant I spins. A connecting line between two terms indicates noncommutativity. The observables are enclosed in a double frame. At the top, two possible separations of the Hamiltonian into observed system, perturbation, and environment are indicated.

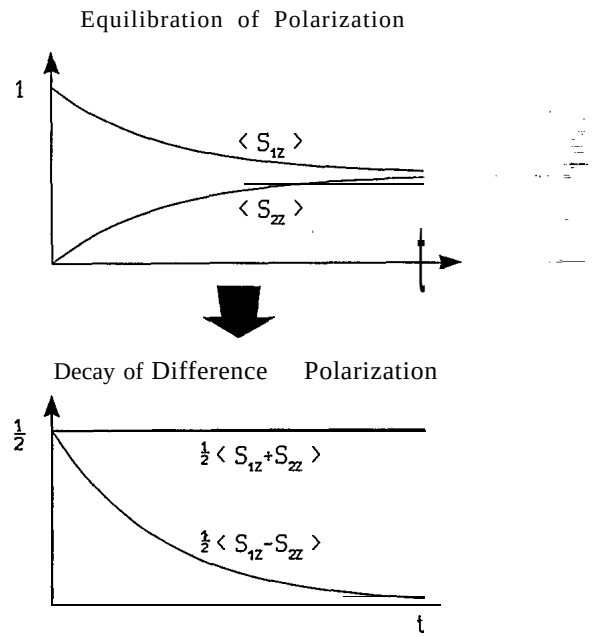

FIG. 3. Relation between the physical exchange process leading to the equilibration of polarization and the treatment in terms of sum and difference polarization used for the calculation of rate wnstants.

between S_1 and S_2 is equivalent to the evolution of a single "difference spin" $S=\frac{1}{2}$, coupled to extraneous I spins and precessing under the influence of a longitudinal field δ and a transverse field with field strength d (in frequency units). As shown in Fig. 3, spin diffusion is equivalent to longitudinal relaxation of this difference spin. The relaxation mechanism is governed by the fluctuating dipolar fields produced by the 1 spins under the influence of their mutual dipole-dipole interaction. This relaxation mechanism has already been suggested by Kronig and Bouwkamp[5,6] for spins at low fields in the laboratory frame. It is also responsible for cross-relaxation effects in the rotating frame.[2–4]

The time evolution of the difference spin is determined by three coupled linear differential equations with three eigenvalues. In the systems to be studied, the transverse components $S_x^{(23)}$ and $S_y^{(23)}$ decay much faster than $S_z^{(23)}$, and the spin diffusion process can be characterized by the decay rate constant of the difference polarization $S_z^{(23)}$ of the two spins S_1 and S_2. The commutation diagram in Fig. 2 suggests two possibilities for selecting the perturbation $\mathcal{H}_1$. We will treat both cases separately.

1. S-spin dipolar interaction considered as the perturbation

The Hamiltonian is separated into the two parts:

$$\mathcal{H}_0=\delta S_z^{(23)}+2\sum_i b_i S_z^{(23)} I_{iz}+\mathcal{H}_{II}^{(23)}\,,\qquad \mathcal{H}_1=-dS_x^{(23)}\,. \tag{21}$$

In this case there is only one relevant observable $S_z^{(23)}$. The corresponding coefficient $W_z^{(23)}$ may be calculated from Eq. (13) by setting $A_k=A_i=S_z^{(23)}$:

$$W_z^{(23)}=-id\,(\mathrm{Tr}\{S_{zz}^{(23)^2}\})^{-1}\mathrm{Tr}\{[S_x^{(23)^T}(t),S_z^{(23)}]S_z^{(23)}\}+(\mathrm{Tr}\{S_z^{(23)^2}\})^{-1}d^2\int_0^\infty d\tau\,\mathrm{Tr}\{[S_x^{(23)^T}(t),S_z^{(23)}][S_x^{(23)^T}(t-\tau),S_z^{(23)}]\}\,, \tag{22}$$

where the duplicate lower index is written only once. Since $S_z^{(23)}$ commutes with $\mathcal{H}_0$, the dependence on t under the trace vanishes. The linear term is zero and we obtain

$$W_z^{(23)}=-d^2(\mathrm{Tr}\{S_z^{(23)^2}\})^{-1}\int_0^\infty d\tau\,\mathrm{Tr}\{S_y^{(23)}(0)S_y^{(23)}(\tau)\}d\tau\,, \tag{23}$$

where

$$S_y^{(23)}(\tau)=e^{i\mathcal{H}_0\tau}S_y e^{-i\mathcal{H}_0\tau}\,. \tag{24}$$

The trace expression in Eq. (23) is the correlation function of the zero-quantum coherence of the two S spins. The integral therefore corresponds to the amplitude at zero frequency, $G^{(23)}(0)$, of the symmetrical zero-quantum spectrum $G^{(23)}(\omega)$ with its two peaks centered at $\omega=\pm\delta$,

$$G^{(23)}(\omega)=(\mathrm{Tr}\{S_y^{(23)^2}\})^{-1}\int_0^\infty d\tau\,e^{-i\omega\tau}\mathrm{Tr}\{S_y^{(23)}\exp(-i\mathcal{H}_0\tau)S_y^{(23)}\exp(i\mathcal{H}_0\tau)\}\,. \tag{25}$$

A similar expression has been obtained by Bloembergen *et al.*[7] Introducing the shape function of the zero-quantum resonance line

$$g^{(23)}(\omega)=\mathrm{Tr}\{S_y^{(23)^2}\}^{-1}\int_0^\infty e^{-i\omega\tau}d\tau\,\mathrm{Tr}\{S_y^{(23)}\exp(-i\mathcal{H}_D^{(23)}\tau)S_y^{(23)}\exp(i\mathcal{H}_D^{(23)}\tau)\}\,, \tag{25a}$$

with the dipolar Hamiltonian

$$\mathcal{H}_D^{(23)}=2\sum_i b_i S_z^{(23)} I_{iz}+\mathcal{H}_{II}^{(23)},$$

we may write

$$W_z^{(23)}=-d^2 g^{(23)}(\delta), \tag{26}$$

where $g^{(23)}(\delta)$ represents the line-shape function of the zero-quantum transition, evaluated at an offset δ from resonance. The zero-quantum line shape can be observed via indirect detection by means of 2D spectroscopy as will be shown in Sec. IVC. The spin-diffusion rate constant $W_z^{(23)}$ can therefore be related to observable quantities. Note that the integral of $g^{(23)}(\omega)$ is normalized to unity.

In the following section we will find an explicit expression for $g^{(23)}(\omega)$ and for the dependence of the transition probability on the offset δ between the two resonance lines.

2. *Heteronuclear dipolar interaction considered as the perturbation*

For the partitioning of the Hamiltonian

$$\mathcal{H}_0=\delta S_z^{(23)}-dS_x^{(23)}+\mathcal{H}_{II}^{(23)},$$
$$\mathcal{H}_1=2\sum_i b_i S_z^{(23)} I_{iz}, \tag{27}$$

we can no longer restrict our attention to the density operator term $S_z^{(23)}$. It does not commute with $\mathcal{H}_0$ and therefore does not represent a quasi-invariant. Furthermore, we note that $\mathcal{H}_1$ commutes with $S_z^{(23)}$ and the approximate procedure of Sec. II B 1 is not applicable to this partitioning. It is necessary to calculate the time evolution of all three components of the density operator. We use in the expansion of the density operator, Eq. (9), the set of operators

$$A_x=S_x^{(23)},\quad A_y=S_y^{(23)},\quad A_z=S_z^{(23)}. \tag{28}$$

In the limit of weak S_1-S_2 interaction $d \ll \delta, (T_2^{ZQT})^{-1}$ (where ZQT represents zero-quantum transition), the calculation may be simplified. All cross terms vanish and

$$\frac{\dot{a}_x(t)}{a_x(t)}=\frac{\dot{a}_y(t)}{a_y(t)}=W_x^{(23)}=W_y^{(23)}=-\frac{1}{T_2^{ZQT}}, \tag{29}$$

$$\dot{a}_z(t)\simeq 0. \tag{30}$$

The transition probability and therefore the relaxation time may be calculated from Eqs. (13) and (27):

$$(T_2^{ZQT})^{-1}=(\mathrm{Tr}\{S_x^{(23)2}\})^{-1}\left[2i\sum_i b_i \mathrm{Tr}\{e^{i\mathcal{H}_{II}t} I_{iz} e^{-i\mathcal{H}_{II}t}[S_z^{(23)},S_x^{(23)}]S_x^{(23)}\}\right.$$
$$\left.-4\sum_i\sum_k b_i b_k \int_0^\infty d\tau\, \mathrm{Tr}\{I_{iz} e^{i\mathcal{H}_{II}\tau} I_{kz} e^{-i\mathcal{H}_{II}\tau}[S_z^{(23)},S_x^{(23)}]^2\}\right]. \tag{31}$$

While the linear term in Eq. (31) clearly vanishes, the quadratic term is equal to

$$(T_2^{ZQT})^{-1}=4(\mathrm{Tr}\{1\})^{-1}\sum_i\sum_k b_i b_k \int_0^\infty d\tau\, \mathrm{Tr}\{I_{iz} e^{i\mathcal{H}_{II}\tau} I_{kz} e^{-i\mathcal{H}_{II}\tau}\}. \tag{32}$$

We now expand the density operator in the laboratory frame,

$$\sigma(t)=e^{-i\mathcal{H}_0 t}\sigma^I(t)e^{i\mathcal{H}_0 t}, \tag{33}$$

in terms of the same operators,

$$\sigma(t)=x(t)S_x^{(23)}+y(t)S_y^{(23)}+z(t)S_z^{(23)}, \tag{34}$$

and obtain the system of differential equations

$$\begin{vmatrix}\dot{x}\\ \dot{y}\\ \dot{z}\end{vmatrix}=\begin{vmatrix}-\frac{1}{T_2^{ZQT}} & -\delta & 0\\ +\delta & -\frac{1}{T_2^{ZQT}}-d & \\ 0 & +d & 0\end{vmatrix}\begin{vmatrix}x\\ y\\ z\end{vmatrix}. \tag{35}$$

We may determine the eigenvalues and eigenvectors of this system of equations. An analytic solution exists in the limit of small d. The eigenvectors are then close to $S_+^{(23)}$, $S_+^{(23)}$, and $S_-^{(23)}$, and

$$\frac{\dot{z}(t)}{z(t)}=W_z^{(23)}=-\frac{1}{T_{SD}}=-\frac{d^2}{(1/T_2^{ZQT})^2+\delta^2}\frac{1}{T_2^{ZQT}}, \tag{36}$$

where T_{SD} represents the spin-diffusion time constant. T_2^{ZQT} is given by Eq. (32).

3. *Comparison of the two approaches*

To compare Eq. (36) with the result of Sec. II B 1, we need an analytic expression for the line shape of the zero-quantum transition. In Sec. II B 2 it has been found that under conditions for which the perturbation expansion converges the zero-quantum coherence decays exponen-

tially. This implies a Lorentzian line shape. With Eq. (26), we find then

$$W_z^{(23)} = -\frac{d^2}{(1/T_2^{ZQT})^2+\delta^2}\frac{1}{T_2^{ZQT}}, \tag{37}$$

which is identical to Eq. (36). That both approaches yield the same result is not astonishing since both involve similar approximations: approach (1),

$$|d| \ll ||\mathcal{H}_{IS}|| \ll ||\mathcal{H}_{II}|| \tag{38}$$

and approach (2),

$$|d| \ll (T_2^{ZQT})^{-1},\ ||\mathcal{H}_{IS}|| \ll ||\mathcal{H}_{II}||,$$

respectively. Systems where Eq. (37) is to be valid have to fulfill the inequalities

$$||\mathcal{H}_{SS}|| < ||\mathcal{H}_{IS}|| < ||\mathcal{H}_{II}|| . \tag{39}$$

From the time dependence of the difference magnetization,

$$\langle S_{1z}-S_{2z}\rangle(t) = \langle S_{1z}-S_{2z}\rangle(0)e^{W_z^{(23)}t}, \tag{40}$$

it is straightforward to calculate the evolution of the polarization of the individual spins. Neglecting spin-lattice relaxation effects, we find

$$\langle S_{1z}\rangle(t) = \tfrac{1}{2}[\langle S_{1z}+S_{2z}\rangle(0)+\langle S_{1z}-S_{2z}\rangle(0)e^{W_z^{(23)}t}],$$
$$\langle S_{2z}\rangle(t) = \tfrac{1}{2}[\langle S_{1z}+S_{2z}\rangle(0)-\langle S_{1z}-S_{2z}\rangle(0)e^{W_z^{(23)}t}] . \tag{41}$$

C. Spectral spin diffusion between two spins S = 1 in the presence of abundant I spins

We assume that two spins S = 1 have identical chemical shifts but differ in their quadrupolar coupling frequencies q_1 and q_2. The Hamiltonian is

$$\mathcal{H} = q_1(S_{1z}^2-\tfrac{2}{3}\mathbb{1})+q_2(S_{2z}^2-\tfrac{2}{3}\mathbb{1}) + d[2S_{1z}S_{2z}-\tfrac{1}{2}(S_1^+S_2^-+S_1^-S_2^+)]+\mathcal{H}_{IS}+\mathcal{H}_{II} . \tag{42}$$

This expression can, in analogy to the preceding section, be rewritten in terms of virtual spin-$\frac{1}{2}$ and virtual spin-1 operators. Terms which commute with all relevant operators will again be neglected:

$$\mathcal{H} = \delta_q S_z^{(23)} - 2dS_x^{(23)} + 2\sum_i b_i S_z^{(23)} I_{iz} + \delta_q S_z^{(78)} - 2dS_x^{(78)} + 2\sum_i b_i S_z^{(78)} I_{iz} + (\sigma_q - 2d)[S_z^{(456)2} - \tfrac{2}{3}\mathbb{1}] - \sqrt{2}dS_x^{(456)} + 2\sum_i b_i S_z^{(456)} I_{iz} + 4\sum (b_{1i}+b_{2i}) S_z^{(19)} I_{iz} + \mathcal{H}_{II} , \tag{43}$$

with

$$\delta_q = (q_1-q_2),\quad \sigma_q = (q_1+q_2),$$
$$b_i = (b_{1i}^{SI}-b_{2i}^{SI}) . \tag{44}$$

The energy-level diagram of the two spins S = 1 is shown in Fig. 4, and Fig. 5 illustrates the resulting networks of noncommuting terms of the Hamiltonian. The system contains in this case three relevant independent subsystems. The subsystems $S^{(23)}$ and $S^{(78)}$ correspond to virtual spin-$\frac{1}{2}$ systems, while $S^{(456)}$ represents a virtual spin-1 system. The virtual Zeeman interaction of the spins-$\frac{1}{2}$ is determined by the difference of the two quadrupolar interactions, while for the spin 1, an effective quadrupolar interaction results which is given by the sum of the quadrupolar interactions of the individual spins and by their dipolar interaction.

The time dependence of the population differences in this system can be described with the four rate constants $W_z^{(23)}$, $W_z^{(78)}$, $W_z^{(456)}$, and $W_{z^2}^{(456)}$. The first two rate con-

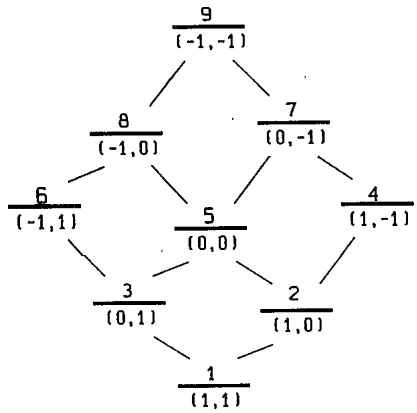

FIG. 4. Energy-level scheme for two spins S = 1, indicating the numbering used in the text.

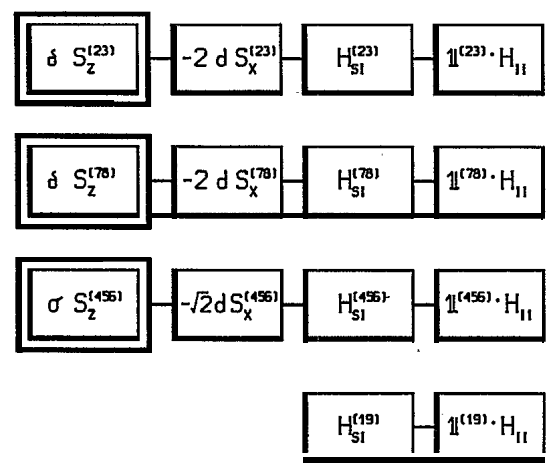

FIG. 5. Commutation diagram for two spins S = 1. A connecting line between two terms indicates noncommutativity. The observables are enclosed in double frames.

stants have the same value due to the symmetry of Eq. (43). It can easily be shown that for large quadrupolar interactions $|q_1|, |q_2| \gg |q_1 - q_2|$ *only* one of the two types of diffusion rates, $W_z^{(23)}, W_z^{(78)}$ or $W_z^{(456)}, W_{z^2}^{(456)}$, *can* be appreciable. For quadrupolar frequencies q_1 and q_2 of equal sign, $W_z^{(23)} = W_z^{(78)}$ can be large, while for quadrupolar frequencies of opposite sign only the virtual spin-1 rate constants $W_z^{(456)}, W_{z^2}^{(456)}$ can be appreciable.

I. *(2,3),(7,8) subsystems*

The terms of the Hamiltonian of Eq. (43) relevant for the (2,3) subsystem are

$$\mathcal{H}^{(23)} = \delta_q S_z^{(23)} - 2dS_x^{(23)} + 2\sum_i b_i S_z^{(23)} I_{iz} + \mathcal{H}_{II}^{(23)} . \tag{45}$$

Apart from a factor 2, this Hamiltonian is identical to Eq. (19). We may therefore directly write down the resulting rate constant,

$$W_z^{(23)} = W_z^{(78)} = -4d^2 g^{(23)}(\delta_q) = -\frac{4d^2/T_2^{ZQT}}{(1/T_2^{ZQT})^2 + \delta_q^2} . \tag{46}$$

2. *(4,5,6) subsystem*

The Hamiltonian for this system is

$$\mathcal{H}^{(456)} = \sigma_q [S_z^{(456)2} - \tfrac{2}{3}\mathbb{1}] - \sqrt{2}dS_x^{(456)} + 2\sum_i b_i S_z^{(456)} I_{iz} + \mathcal{H}_{II}^{(456)} , \tag{47}$$

where we have neglected d as compared to σ_q. Perturbation theory shall be applied in analogy to Sec. II B 1. The diagonal part of the virtual spin-l density operator is expanded in terms of three orthogonal operators:

$$A_z = S_z^{(456)}, \quad A_{z^2} = S_z^{(456)2} - \tfrac{2}{3}\mathbb{1}^{(456)}, \quad A_1 = \mathbb{1} ,$$

which leads to the expansion

$$\sigma^{(456)} = a_z A_z + a_{z^2} A_{z^2} . \tag{48}$$

With the perturbation $\mathcal{H}_1$ chosen as $-\sqrt{2}dS_x^{(456)}$, we can calculate the rate constant of Zeeman order $W_z^{(456)}$ from Eq. (13):

$$W_z^{(456)} = (\mathrm{Tr}\{S_z^{(456)2}\})^{-1} \left[-i\mathrm{Tr}\{[-\sqrt{2}dS_x^{(456)}(t), S_z^{(456)}] S_z^{(456)}\} + \int_0^\infty 2d^2 \mathrm{Tr}\{[S_x^{(456)}(t), S_z^{(456)}][S_x^{(456)}(t-\tau), S_z^{(456)}]\} d\tau \right]$$
$$= -2d^2 (\mathrm{Tr}\{S_z^{(456)2}\})^{-1} \int_0^\infty \mathrm{Tr}\{S_y^{(456)}(0) S_y^{(456)}(\tau)\} d\tau . \tag{49}$$

As in the spin-+ case [Eq. (23)], this may be written in terms of the zero-quantum line shape $g^{(456)}(\omega)$:

$$W_z^{(456)} = -2d^2 g^{(456)}(\sigma_q) , \tag{50}$$
$$g^{(456)}(\omega) = \mathrm{Tr}\{S_y^{(456)2}\}^{-1} \int_0^\infty e^{-i\omega\tau} d\tau \, \mathrm{Tr}\{S_y^{(456)} \exp(-i\mathcal{H}_D^{(456)}\tau) S_y^{(456)} \exp(i\mathcal{H}_D^{(456)}\tau)\}$$

and

$$\mathcal{H}_D^{(456)} = 2\sum_i b_i S_z^{(456)} I_{iz} + \mathcal{H}_{II}^{(456)} .$$

In a similar manner we may calculate the relaxation of quadrupolar order A_{z^2}. The linear term vanishes again and we find

$$W_{z^2}^{(456)} = [\mathrm{Tr}\{(S_z^{(456)2} - \tfrac{2}{3}\mathbb{1})^2\}]^{-1} \int_0^\infty 2d^2 \mathrm{Tr}\{[S_x^{(456)}(t), S_z^{(456)2}][S_x^{(456)}(t-\tau), S_z^{(456)2}]\} d\tau \tag{51}$$
$$= -[\mathrm{Tr}\{(S_z^{(456)2} - \tfrac{2}{3}\mathbb{1})^2\}]^{-1} \int_0^\infty d\tau 2d^2 \mathrm{Tr}\{(S_z^{(456)} S_y^{(456)}(0) + S_y^{(456)}(0) S_z^{(456)})(S_z^{(456)} S_y^{(456)}(\tau) + S_y^{(456)}(\tau) S_z^{(456)})\} . \tag{52}$$

The trace represents antiphase zero-quantum coherence and we may again express the integral by the amplitude at zero frequency of the zero-quantum spectrum, leading to

$$W_{z^2}^{(456)} = -6d^2 g^{(456)}(\sigma_q) . \tag{53}$$

The operators A_z and A_{z^2} have been chosen for the expansion of the density operator because the cross terms $W_{zz^2}^{(456)}$ and $W_{z^2z}^{(456)}$ vanish. This can be demonstrated by considering the symmetry transformation

$$U = \exp\left\{ i\pi \left[S_x^{(456)} + \sum_i I_{ix} \right] \right\} ,$$

which leaves $\mathcal{H}^{(456)}$ invariant. However, the operators A_z and A_{z^2} transform differently,

$$U^{-1} A_z U = -A_z, \quad U^{-1} A_{z^2} U = A_{z^2} , \tag{54}$$

and do not mix under the symmetric Hamiltonian $\mathcal{H}^{(456)}$, so that $W_{z^2z}^{(456)} = W_{zz^2}^{(456)} = 0$. Equations (50) and (53) show

that the expectation values of the two operators A_z, A_{z^2} decay with different rates, although the mechanism which causes the relaxation is the same for both. This has been confirmed experimentally and will be discussed in the context of the experimental results. Equations (50) and (51) do not give an explicit offset dependence of the rate constants. Similar to the $S=\frac{1}{2}$ case, we expect that for a large class of systems the dependence of the rate constants $W_z^{(456)}$ and $W_{z^2}^{(456)}$ on the frequency difference of the two spins S_1 and S_2 will be Lorentzian.

3. *Double-quantum mechanism of spin diffusion for two spins S=1*

It has been mentioned that spin diffusion between two spins S = 1 proceeds independently in three subsystems, one of which is the three-level system (4,5,6) with two degenerate energy levels 4 and 6 (neglecting chemical shift differences). It has been shown in Sec. II C2 that spin diffusion within this subsystem proceeds via the transitions (4,5) and (5,6) (see Fig. 4), which are both bridged by a perturbation term $2dS_x^{(55)}$ and $2dS_x^{(56)}$, respectively. It has been suggested[24,25] that an additional mechanism may transfer population directly between the degenerate levels 4 and 6. Because the dipole interaction does not include a matrix element between these two states, this must be a higher-order process. It may be called "double-quantum spin diffusion" because it corresponds to the simultaneous exchange of two quanta between the two spins in contrast to the processes which have been considered so far, where only one quantum is exchanged.

The relevant Hamiltonian of Eq. (43), written in terms of single transition operators, is

$$\mathcal{H}^{(456)}=S_z^{(45)}\left[\tfrac{2}{3}\sigma_q+4\sum_i b_i I_{iz}\right]+S_z^{(65)}\left[\tfrac{2}{3}\sigma_q-4\sum_i b_i I_{iz}\right]-2d(S_x^{(45)}+S_x^{(65)})\,. \tag{55}$$

This system is equivalent to a single spin $S=1$, irradiated on resonance with a rf field of strength $\sqrt{2}d$ which excites the double-quantum transition occurring in the center between the two single-quantum transitions. By second-order perturbation theory, it is possible to reduce the three-level Hamiltonian of Eq. (55) to a two-level Hamiltonian describing exclusively the double-quantum transition:[30]

$$\mathcal{H}^{(46)}=d'S_x^{(46)}+4\sum b_i I_{iz}S_z^{(46)}+\mathcal{H}_{II}^{(46)}$$

with the effective dipolar coupling constant

$$d'=\frac{2d^2}{\sigma_q}\,. \tag{56}$$

The problem is now equivalent to the spin-$ case treated in Sec. IIB. By analogy we find the result

$$W_z^{(46)}=d'^2 g^{(46)}(0)=\frac{4d^4}{\sigma_q^2}g^{(46)}(0)\,, \tag{57}$$

where $g^{(46)}(\omega)$ represents the line-shape function of the (4,6) transition. This shows that the double-quantum spin-diffusion rate is inversely proportional to the square of the sum of the two quadrupolar frequencies q_1+q_2. While for equal signs, a negligible double-quantum spin-diffusion rate is expected, it can become significant for opposite signs. This behavior is similar to that of the single-quantum processes in the (4,5,6) subsystem. The rates of the two processes differ by

$$\frac{W_z^{(456)}}{W_z^{(46)}}=\frac{-2d^2g^{(45)}(\sigma_q)\sigma_q^2}{-4d^4g^{(46)}(0)}\,. \tag{58}$$

If the heteronuclear dipolar *IS* couplings are much weaker than the *II* interactions, we expect as in the case of two spins $\frac{1}{2}$ a tendency towards Lorentzian line shapes due to the averaging effect of the strong *II* interactions on the *IS* couplings which determine the line shape. According to Eq. (31), the transverse relaxation times will be related by

$$\frac{T_2^{(46)}}{T_2^{(45)}}=\frac{\mathrm{Tr}\{[S_z^{(456)},S_x^{(45)}]^2\}\mathrm{Tr}\{S_x^{(46)^2}\}}{\mathrm{Tr}\{S_x^{(45)^2}\}\mathrm{Tr}\{[S_z^{(456)},S_x^{(46)}]^2\}}=\frac{1}{4}\,,$$

and therefore

$$\frac{W_z^{(456)}}{W_z^{(46)}}=\frac{2\sigma_q^2}{d^2[1+T_2^{(45)^2}\sigma_q^2]}\,. \tag{59}$$

The implications of this formula can easily be understood by evaluating the two limiting cases of well resolved and strongly overlapping resonance lines. For $\sigma_q^2 T_2^{(45)^2}\gg 1$, we find

$$\frac{W_z^{(456)}}{W_z^{(46)}}=\frac{2}{d^2T_2^{(45)^2}}\,. \tag{60}$$

In the other extreme, $\sigma_q^2 T_2^{(45)^2}\ll 1$,

$$\frac{W_z^{(456)}}{W_z^{(46)}}=\frac{2\sigma_q^2}{d^2}\,. \tag{61}$$

These two cases imply that under conditions where the perturbation treatment is valid, the double-quantum mechanism will always be negligible compared to the single-quantum process. It may however become appreciable when the dipolar coupling d is so large that the second-order perturbation treatment starts to fail and the fourth-order terms become important. This situation will be discussed in the experimental Sec. VI.

4. *Time dependence of measurable quantities*

A spin-diffusion measurement does not access directly the quantities whose time dependence has been calculated with the perturbation treatment. Instead, the polarizations of the spins S_1 and S_2 are measured. The time dependence of these observables is in general nonexponential. For two isolated spins, the transitions in the (2,3), (4,5,6), and (7,8) systems are independent; the three difference spins relax independently. If the system is initially in a state

$$\sigma(0)=a_1(0)S_{1z}+a_2(0)S_{2z}+b_1(0)(S_{1z}^2-\tfrac{2}{3}\mathbb{1}) + b_2(0)(S_{2z}^2-\tfrac{2}{3}\mathbb{1}) , \quad (62)$$

the expectation values will evolve as

$$\langle S_{1z}\rangle(t)=\tfrac{1}{2}s_a+\tfrac{1}{12}d_a(e^{W_z^{(23)}t}+e^{W_z^{(78)}t}+4e^{(W_z^{(456)}+W_z^{(46)})t}) ,$$
$$\langle S_{2z}\rangle(t)=\tfrac{1}{2}s_a-\tfrac{1}{12}d_a(e^{W_z^{(23)}t}+e^{W_z^{(78)}t}+4e^{(W_z^{(456)}+W_z^{(46)})t}) , \quad (63)$$
$$\langle S_{1z}^2-\tfrac{2}{3}\mathbb{1}\rangle(t)=\tfrac{1}{6}s_b(1+2e^{W_{z^2}^{(456)}t}) + \tfrac{1}{4}d_b(e^{W_z^{(23)}t}+e^{W_z^{(78)}t}) ,$$
$$\langle S_{2z}^2-\tfrac{2}{3}\mathbb{1}\rangle(t)=\tfrac{1}{6}s_b(1+2e^{W_{z^2}^{(456)}t}) - \tfrac{1}{4}d_b(e^{W_z^{(23)}t}+e^{W_z^{(78)}t}) ,$$

with

$$s_a=a_1(0)+a_2(0),\quad d_a=a_1(0)-a_2(0) , \quad (64)$$
$$s_b=b_1(0)+b_2(0),\quad d_b=b_1(0)-b_2(0) .$$

Here s_a and d_a represent sum and difference of the Zeeman orders, while s_b and d_b represent sum and difference of the quadrupole orders of the two spins S_1 and S_2.

Usually the two spins are not isolated from the other S spins. If the contact between spins of the same type (e.g., S_1-S_1) is of the same strength as that between the two different types (i.e., S_1-S_2), the evolution of the system depends also on the S_i-S_i rates. In many cases the spin diffusion among equivalent spins is much faster than between nonequivalent spins, so that each class of equivalent spins represents a thermal bath in internal equilibrium. The density operator can then at all times be described by an expansion of the type of Eq. (62). The coefficients show the following time dependence:

$$a_1(t)=\tfrac{1}{2}[s_a+d_a\exp(-t/T_{SD}^{Z})] ,$$
$$a_2(t)=\tfrac{1}{2}[s_a-d_a\exp(-t/T_{SD}^{Z})] ,$$
$$b_1(t)=\tfrac{1}{2}[s_b\exp(-t/T_{SD}^{Q\Sigma})+d_b\exp(-t/T_{SD}^{Q\Delta})] , \quad (65)$$
$$b_2(t)=\tfrac{1}{2}[s_b\exp(-t/T_{SD}^{Q\Sigma})-d_b\exp(-t/T_{SD}^{Q\Delta})] ,$$

with the diffusion rate constant of Zeeman order

$$1/T_{SD}^{Z}=-\tfrac{1}{6}[W_z^{(23)}+W_z^{(78)}+4(W_z^{(456)}+W_z^{(46)})] , \quad (66a)$$

the decay rate constant of the difference of quadrupolar order

$$1/T_{SD}^{Q\Delta}=-\tfrac{1}{2}(W_z^{(23)}+W_z^{(78)}) , \quad (66b)$$

and with the decay rate constant of the sum of quadrupolar order

$$1/T_{SD}^{Q\Sigma}=-\tfrac{2}{3}W_{z^2}^{(456)} . \quad (66c)$$

If the quadrupolar frequencies q_1 and q_2 significantly exceed their difference $|q_1|,|q_2| \gg |q_1|-|q_2|$, then spin diffusion occurs exclusively in the (2,3) and (7,8) subsystems or exclusively in the (4,5,6) subsystem, depending on the relative signs of q_1 and q_2. In the case that single-quantum spin diffusion dominates and the double-quantum process $W_z^{(46)}$ *can* be neglected, we find for the diffusion rate constant of Zeeman order

$$1/T_{SD}^{Z}=\tfrac{4}{3}d^2g(\Delta\omega) , \quad (66d)$$

with the line-shape function g (ω) of the transitions (23),(78) and (4,5),(5,6) and with the separation $\Delta\omega=|q_1|-|q_2|$ of the two peaks involved in the spin-diffusion process. This result applies irrespective of the relative signs of q_1 and q_2, as has been found experimentally."

The rate constants for diffusion of quadrupolar order, on the other hand, depend on the relative sign: for equal signs,

$$1/T_{SD}^{Q\Delta}=4d^2g(\Delta\omega),\quad 1/T_{SD}^{Q\Sigma}\simeq 0 , \quad (66e)$$

and for opposite signs,

$$1/T\&O,\quad 1/T_{SD}^{Q\Sigma}=4d^2g(\Delta\omega) . \quad (66f)$$

Quadrupolar order of spin S_1 is in the first case transferred into quadrupolar order of the same sign for spin S_2, in the second case into quadrupolar order of opposite sign for spin S_2. It should, however, be noted that the resulting 2D spectra are indistinguishable and that the observed spin-diffusion rate, which corresponds in the first case to $1/T_{SD}^{Q\Delta}$ and in the second case to $1/T_{SD}^{Q\Sigma}$, does not depend on the relative sign of the coupling constants. The transfer of quadrupolar order is predicted to be three times faster than the transfer of Zeeman order.

Double-quantum spin diffusion occurs exclusively for opposite signs of the quadrupolar frequencies q_1 and q_2 and thus provides a means to determine relative signs. We expect that for double-quantum spin diffusion only Zeeman order is transferred and no quadrupolar order. If the diffusion of Zeeman and quadrupolar order is measured independently, it is therefore possible to distinguish single-quantum and double-quantum processes.

D. Spectral spin diffusion in homonuclear spin systems

The treatment of spin diffusion in homonuclear spin systems is in general more complicated than spin diffusion in heteronuclear systems. In the preceding section, we took advantage of the clear distinction between the dipolar interaction of the diffusion partners, which had very little heat capacity, and the dipolar interaction to and among the 1 spins which was essential for the energy balance within the system. In homonuclear systems, the coupling between diffusion partners and the energy balance are both achieved by the homonuclear dipolar interaction.

In some cases, we may nevertheless apply the perturbation treatment developed for the heteronuclear case. We assume that the solid contains two S-spin species S_1 and S_2, contributing to separate resonance lines, with strong dipolar couplings within each species and with weaker dipolar coupling between the species as illustrated in Fig. 6. Such a situation is approximated by malonic acid—d_4, where the coupling among the methylene deuterons and among the carboxyhc deuterons is larger than the cou-

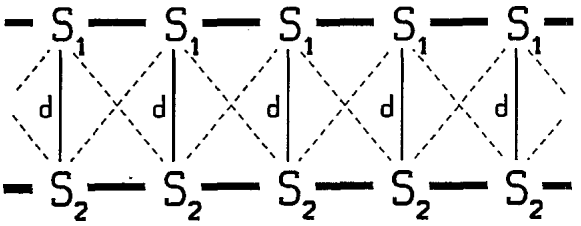

FIG. 6. Schematic representation of spin diffusion in homonuclear systems, visualizing the assumption made in the text: The couplings within each spin species are assumed to be stronger than between them. Only one type of coupling (solid vertical lines) is taken into account. The other couplings (dashed lines) can be treated in the same way since cross terms between different interactions vanish in the second-order perturbation treatment.

plings between them. The formal similarity to the heteronuclear case is then preserved. The intra-species interaction serves as a heat reservoir while the inter-species dipolar interaction d can be treated as a perturbation, neglecting its heat capacity. Within second-order perturbation theory, we can limit ourselves to one type of inter-species interaction. The remaining interactions can be treated analogously and give additive contributions to the spin-diffusion rate.

The system may then be described by the Hamiltonian

$$\mathcal{H}=\mathcal{H}_z^{(1)}+\mathcal{H}_z^{(2)}+\mathcal{H}_d^{(12)}+\mathcal{H}_d^{(11)}+\mathcal{H}_d^{(22)}\,, \tag{67}$$

with

$$\mathcal{H}_z^{(i)}=\Omega_i\sum_k S_{kz}^{(i)}\,,$$

$$\mathcal{H}_d^{(12)}=d\sum_k[2S_{kz}^{(1)}S_{kz}^{(2)}-\tfrac{1}{2}(S_k^{(1)+}S_k^{(2)-}+S_k^{(1)-}S_k^{(2)+})]\,, \tag{68}$$

$$\mathcal{H}_d^{(ii)}=\sum_l\sum_{\substack{k\\k<l}} b_{kl}^{(ii)}[2S_{kz}^{(i)}S_{lz}^{(i)}-\tfrac{1}{2}(S_k^{(i)+}S_l^{(i)-}+S_k^{(i)-}S_l^{(i)+})]\,,$$

$$i=1,2\,.$$

Because the total z component $\sum_k[S_{kz}^{(1)}+S_{kz}^{(2)}]$ commutes with the full Hamiltonian, we can introduce again sum and difference frequency Hamiltonians

$$\mathcal{H}^{\Sigma}=(\Omega_1+\Omega_2)\tfrac{1}{2}\sum_k[S_{kz}^{(1)}+S_{kz}^{(2)}]\,,$$

$$\mathcal{H}^{\Delta}=(\Omega_1-\Omega_2)\tfrac{1}{2}\sum_k[S_{kz}^{(1)}-S_{kz}^{(2)}]=(\Omega_1-\Omega_2)S_z^{(23)}\,. \tag{69}$$

$\mathcal{H}^{\Sigma}$ is a constant of motion and can be disregarded in the following. We may now make the selection

$$\mathcal{H}_0=\mathcal{H}^{\Delta}+\mathcal{H}_d^{(11)}+\mathcal{H}_d^{(22)},\quad \mathcal{H}_1=\mathcal{H}_d^{(12)}\,, \tag{70}$$

and apply Eq. (13) to obtain an expression for the expectation value of the difference polarization $S_z^{(23)}$:

$$\frac{d}{dt}\langle S_z^{(23)}\rangle=W_z^{(23)}\langle S_z^{(23)}\rangle\,, \tag{71}$$

with

$$W_z^{(23)}=-\frac{d^2}{\mathrm{Tr}\{S_z^{(23)2}\}}\int_0^{\infty}d\tau\,\mathrm{Tr}\{S_y^{(23)}(0)S_y^{(23)}(\tau)\}\,, \tag{72}$$

where

$$S_y^{(23)}=-\tfrac{1}{2}i\sum_k(S_k^{(1)+}S_k^{(2)-}-S_k^{(1)-}S_k^{(2)+}) \tag{73}$$

and

$$S_y^{(23)}(\tau)=e^{i\mathcal{H}_0\tau}S_y^{(23)}e^{-i\mathcal{H}_0\tau} \tag{74}$$

This result is formally equivalent to Eq. (23) for the heteronuclear case. However, the explicit evaluation to obtain the offset dependence of $W_z^{(23)}$ is far from trivial.

The two perturbation treatments in Secs. II B 1 and II B 2 diverge in their predictions. Approach (1) predicts a rate constant $W_z^{(23)}$ proportional to $g^{(23)}(\Omega_1-\Omega_2)$. The offset dependence should therefore deviate from the inverse quadratic behavior when the Lorentzian form is no longer an adequate description of the line shape. This must arise at some offset, determined by the finite second moment of the particular system. Approach (2), on the other hand, predicts the inverse square law to hold as long as the envelope of the free induction decay (FID) is exponential. It has been shown[31] that the long-time asymptotic form of the FID is exponential under certain conditions. Approach (2) would therefore suggest that the inverse square law holds even for large offsets.

III. THERMODYNAMICS OF SPECTRAL SPIN DIFFUSION

The ultimate equilibrium state reached after a sufficiently long spin-diffusion period is determined by thermodynamics rather than by the spin-diffusion rate constants calculated in Sec. II. The principles of energy conservation and of equal spin temperatures in thermal equilibrium easily allow the computation of the equilibrium state if the finite heat capacity of the environment is taken into account.

We divide again the Hamiltonian into the relevant part $\mathcal{H}_S$, representing a difference term, the external degrees of freedom $\mathcal{H}_E$, and the interaction term $\mathcal{H}_{SE}$,

$$\mathcal{H}=\mathcal{H}_S+\mathcal{H}_E+\mathcal{H}_{SE}\,. \tag{75}$$

In the high-temperature approximation, the quasiequilibrium density operator may be written in the form

$$\sigma=(1-\beta_S\mathcal{H}_S-\beta_E\mathcal{H}_E)/\mathrm{Tr}\{1\}\,, \tag{76}$$

with the inverse spin temperatures β_S and β_E, neglecting the heat capacity of the interaction term $\mathcal{H}_{SE}$. The total spin energy of the system, expressed by the initial density operator, is given by

$$\langle\mathcal{H}\rangle^i=-\beta_S^i\mathrm{Tr}\{\mathcal{H}_S^2\}-\beta_E^i\mathrm{Tr}\{\mathcal{H}_E^2\}$$
$$=-\beta_S^iC_S-\beta_E^iC_E\,, \tag{77}$$

with the heat capacities $C_S=\mathrm{Tr}\{\mathcal{H}_S^2\}$ and $C_E=\mathrm{Tr}\{\mathcal{H}_E^2\}$.

In the course of spin diffusion, the two spin temperatures are equalized leading to the final state

$$\sigma^f=[1-\beta^f(\mathcal{H}_S+\mathcal{H}_E)]/\mathrm{Tr}\{1\}\ , \tag{78}$$

with the final inverse spin temperature

$$\beta^f=\frac{\beta_S^i C_S+\beta_E^i C_E}{C_S+C_E}\ . \tag{79}$$

This expression can easily be generalized to systems with more than one relevant term $\mathcal{H}_{Sk}$,

$$\sigma=\left[1-\sum_k \beta_{Sk}\mathcal{H}_{Sk}-\beta_E\mathcal{H}_E\right]\Big/\mathrm{Tr}\{1\}\ , \tag{80}$$

with the final inverse spin temperature

$$\beta^f=\frac{\sum_k \beta_{Sk}^i C_{Sk}+\beta_E^i C_E}{\sum_k C_{Sk}+C_E}\ . \tag{81}$$

A. Two spins $S=\frac{1}{2}$ coupled to a large number of I spins

We start from the Hamiltonian for the difference spin given by Eq. (19), taking $\delta S_z^{(23)}-dS_x^{(23)}$ as the relevant part $\mathcal{H}_S$, and the dipolar interaction of the I spins as the environment $\mathcal{H}_E$. The corresponding heat capacities are

$$C_S=(\delta^2+d^2)\mathrm{Tr}\{S_z^{(23)^2}\}\simeq\delta^2\mathrm{Tr}\{S_z^{(23)^2}\}\ , \tag{82}$$

$$C_E=\mathrm{Tr}\{\mathcal{H}_{II}^2\}\ . \tag{83}$$

For most cases of practical interest, we have

$$C_E\gg C_S\ , \tag{84}$$

which yields from Eq. (79)

$$\beta^f=\beta_E^i\ . \tag{85}$$

It can be assumed that $\beta_E^i=\beta_L$ where β_L is the inverse lattice temperature and therefore the final population difference across the zero-quantum transition (2,3) will be negligibly small, so that in equilibrium the two spins S_1 and S_2 will assume the same polarization; spin diffusion proceeds to completion.

B. Two spins S $=1$ coupled to a large number of I spins

As shown in Sec. II, we have to consider the three relevant terms $S_{1z}-S_{2z}$, $S_{1z}^2-S_{2z}^2$, and $S_{1z}^2+S_{2z}^2-\frac{4}{3}1$ which are in contact with the I-spin dipolar bath. We specialize here for the case where the two quadrupolar coupling constants have the same sign, so that the third term is practically isolated and need not be taken into account. The density operator may be written as

$$\sigma=\left[1-\beta_z(S_{1z}-S_{2z})-\beta_{z^2}(S_{1z}^2-S_{2z}^2)\frac{q_1-q_2}{2}-\beta_{II}\mathcal{H}_{II}\right]\Big/\mathrm{Tr}\{1\}\ , \tag{86}$$

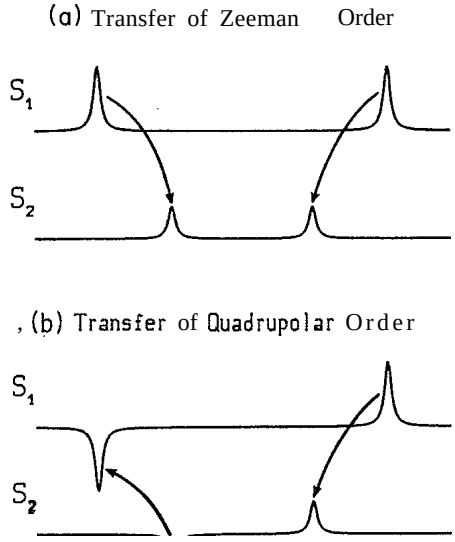

FIG. 7. The amount of energy required for a spin-diffusion step to occur is visualized. (a) In the case of diffusion of Zeeman order, the flow of population proceeds in opposite directions in the two halves of the spectrum and the two contributions to the total energy cancel. (b) In the case of quadrupolar order, the two transitions have opposite population differences and the flow of energy is additive.

where all invariant terms have been omitted. The corresponding heat capacities are

$$C_z=0,\quad C_{z^2}=\tfrac{1}{9}(q_1-q_2)^2\mathrm{Tr}\{1\},\quad C_{II}=\mathrm{Tr}\{\mathcal{H}_{II}^2\}\ . \tag{87}$$

The relation $C_z=0$ implies that a transfer of Zeeman order between the two spins does not require an energy exchange with the bath. Therefore, the equilibrium Zeeman polarizations of the two S spins are equal, irrespective of the size of the dipolar bath. This is not the case for the quadrupolar order. Here, an amount of energy equal to the difference of the two coupling constants has to be exchanged with the dipolar bath. But also in this case the heat capacity of the dipolar bath is usually large enough to let spin diffusion proceed to completion. The different situations are visualized diagrammatically in Fig. 7.

C. Homonuclear system of spins $S=1$

Equations (86) and (87) of the heteronuclear case may also be applied to the homonuclear case if $\mathcal{H}_{II}$ is replaced by $\mathcal{H}_{SS}=\mathcal{H}_d^{(11)}+\mathcal{H}_d^{(22)}$ and if the condition for the application of perturbation theory if fulfilled. However, the consequences are different. The observation of spectral spin diffusion requires that the separation between the resonance lines, $|q_1-q_2|$, be larger than the linewidth which may be taken as a measure for the size of the dipolar bath, $|\mathcal{H}_{SS}|$, so that we have to require

$$C_{z^2}>C_{SS}\ . \tag{88}$$

This means, according to Eq. (79), that the equilibrium temperature reached does not deviate much from the initial temperature of the quadrupolar bath, so that only a

small amount of quadrupolar energy is taken up by the dipolar interaction and little quadrupolar order may be transferred. This implies that spin diffusion stops before the polarization of the two spins is equalized. The limited heat capacity of the dipolar interaction forms a bottleneck for spin diffusion. It should, however, be taken into account that relaxation with the rate constant $1/T_{1D}$ couples the dipolar bath to the lattice which has a virtually infinite heat capacity. This situation is represented in Fig. 8. The time dependence of the inverse temperatures β_{z^2} and β_{SS} in this enlarged system may be represented as

$$\begin{bmatrix} \dot{\beta}_{z^2} \\ \dot{\beta}_{SS} \end{bmatrix} = \begin{bmatrix} -\frac{1}{T_{SD}^{Q\Delta}} & \frac{1}{T_{SD}^{Q\Delta}} \\ \frac{C_{z^2}}{C_{SS}}\frac{1}{T_{SD}^{Q\Delta}} & -\frac{C_{z^2}}{C_{SS}}\frac{1}{T_{SD}^{Q\Delta}} - \frac{1}{T_{1D}} \end{bmatrix} \begin{bmatrix} \beta_{z^2} \\ \beta_{SS} \end{bmatrix}, \quad (89)$$

with the eigenvalues of the matrix of rate coefficients given by

$$2\lambda_{1,2} = -\left[\frac{1+(C_{z^2}/C_{SS})}{T_{SD}^{Q\Delta}} + \frac{1}{T_{1D}}\right] \pm \left[\frac{[1+(C_{z^2}/C_{SS})]^2}{(T_{SD}^{Q\Delta})^2} - 2\frac{1-(C_{z^2}/C_{SS})}{T_{SD}^{Q\Delta}T_{1D}} + \frac{1}{T_{1D}^2}\right]^{1/2}. \quad (90)$$

For fast relaxation of the dipolar bath,

$$\frac{1}{T_{1D}} \gg \frac{C_{z^2}}{C_{SS}}\frac{1}{T_{SD}^{Q\Delta}},$$

the two eigenvalues become equal to $-(1/T_{SD}^{Q\Delta})$ and $-(1/T_{1D})$ so that in this limit spin diffusion proceeds at the same rate as it would in a system with very large dipolar bath. For intermediate relaxation rates, the diffusion of quadrupolar order will be slowed down, while the diffusion rate of Zeeman order will not be affected. Therefore, a comparison of the two rates gives a measure for the relaxation time T_{1D} of the dipolar bath.

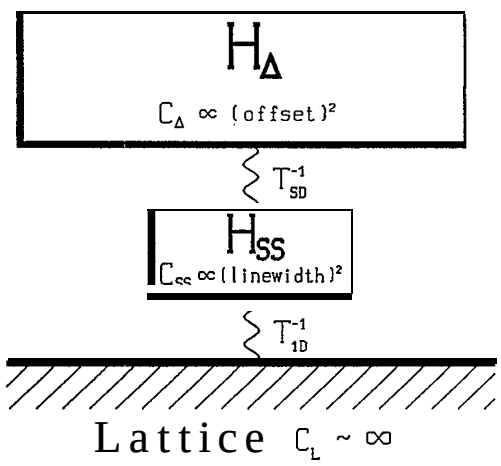

FIG. 8. Schematic representation of the heat reservoirs involved in the thermodynamics of spin diffusion in homonuclear systems. The reservoir $\mathcal{H}_\Delta$ associated with the population difference may have a much larger heat capacity than the dipolar bath $\mathcal{H}_{SS}$. Therefore, a coupling to the lattice is required for spin diffusion to proceed to completion.

IV. MEASUREMENT OF SPIN DIFFUSION IN A SYSTEM WITH TWO SPINS $S=\frac{1}{2}$ COUPLED TO EXTRANEOUS SPINS $I=\frac{1}{2}$

A. Experimental scheme

Spin diffusion represents an exchange-type phenomenon and the measurement techniques are the same as those for the detection of chemical exchange or cross relaxation in liquids. One- or two-dimensional (2D) schemes can be applied. All the experiments described in this paper were performed as two-dimensional experiments. In simple systems, however, one-dimensional experiments can yield similar results. The pulse sequences for the 2D experiments are shown in Fig. 9. They consist basically of the three-pulse sequence originally proposed for exchange studies.[32] In the case of the heteronuclear systems, the first pulse is replaced by a cross-polarization transfer from the I spins. The experiments were performed on a home-built spectrometer equipped with a Varian V71 computer and a Bruker 5.1 T magnet corresponding to a proton resonance frequency of 220 MHz.

B. Evolution of the spin system

Since heteronuclear spin decoupling is applied during the evolution and detection periods, we do not have to consider the terms $\mathcal{H}_{IS}, \mathcal{H}_{II}$ of Eq. (14). To simplify the calculation, we assume that the two mixing pulses in Fig. 9(a) are ideal $\pi/2$ pulses. We may also disregard the S-S dipolar coupling during evolution and detection periods.

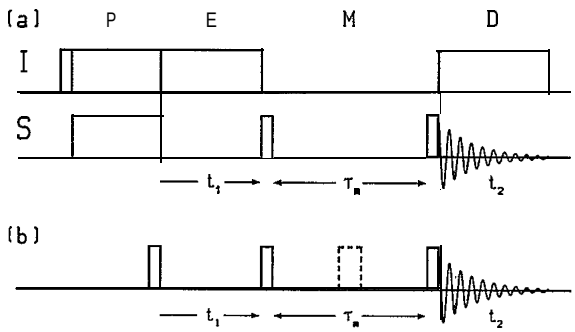

FIG. 9. Schemes for two-dimensional spin-diffusion experiments. (a) In the heteronuclear case, cross polarization is used to create S-spin polarization. During the evolution period, I-spin decoupling is applied. Before the mixing period, a 90° pulse converts one component of the transverse magnetization into polarization. The second mixing pulse is applied to monitor the system after the exchange process has taken place. (b) In the homonuclear case, preparation is achieved by a 90° pulse. The two mixing pulses are 90° pulses if Zeeman order is observed, or 45° pulses for the observation of quadrupolar order. In the latter case, a 180° pulse is inserted in every second scan (indicated by dashed lines) in order to eliminate Zeeman order which may also be present during the mixing period.

It leads to a splitting of the lines in both dimensions as shown in Fig. 10. For ideal $\pi/2$ pulses, the four lines of each multiplet have the same intensity and phase.

After preparation by cross polarization, the carbon spin system is described by the traceless density operator

$$\sigma(0+)=S_{1x}+S_{2x}. \tag{91}$$

During the evolution period, the two spins precess under the Zeeman interaction. The density operator at the end of the evolution period is, neglecting relaxation,

$$\sigma(t_1)=S_{1x}\cos(\Omega_1 t_1)+S_{1y}\sin(\Omega_1 t_1) +S_{2x}\cos(\Omega_2 t_1)+S_{2y}\sin(\Omega_2 t_1). \tag{92}$$

With a $(\pi/2)_{-y}$ pulse as the first mixing pulse, we get

$$\sigma(t_1,0)=S_{1z}\cos(\Omega_1 t_1)+S_{1y}\sin(\Omega_1 t_1) +S_{2z}\cos(\Omega_2 t_1)+S_{2y}\sin(\Omega_2 t_1). \tag{93}$$

The mixing time τ_m is usually considerably longer than the transverse relaxation time T_2, so that all transverse terms such as S_{1y}, S_{2y} die out. The longitudinal terms are conveniently written as sum and difference polarization:

$$\sigma^l(t_1,0)=\tfrac{1}{2}(S_{1z}+S_{2z})[\cos(\Omega_1 t_1)+\cos(\Omega_2 t_1)] +\tfrac{1}{2}(S_{1z}-S_{2z})[\cos(\Omega_1 t_1)-\cos(\Omega_2 t_1)]. \tag{94}$$

As shown in Sec. II B, the first of these terms remains invariant while the second decays under the influence of spin diffusion:

$$\sigma(t_1,\tau_m)=\tfrac{1}{2}(S_{1z}+S_{2z})[\cos(\Omega_1 t_1)+\cos(\Omega_2 t_1)] +\tfrac{1}{2}(S_{1z}-S_{2z})[\cos(\Omega_1 t_1)-\cos(\Omega_2 t_1)] \times e^{W_z^{(23)}\tau_m}. \tag{95}$$

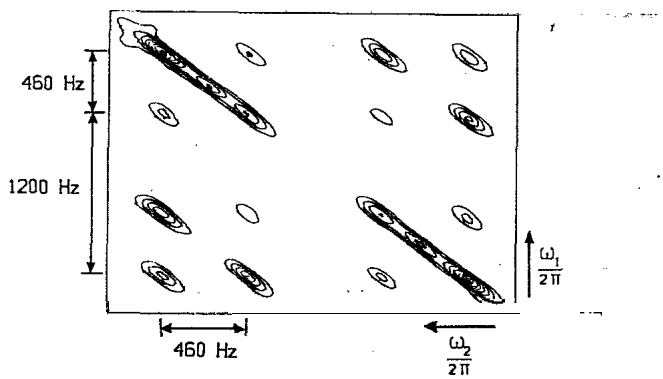

FIG. 10. Two-dimensional spin-diffusion spectrum of a malonic acid—$^{13}C_2$ single crystal (orientation 1). The diagonal shows the one-dimensional (1D) spectrum, consisting of two dipolar doublets. In the center of each doublet the resonance of the singly labeled molecules appears. The cross peaks close to the diagonal connecting the diagonal peaks of the same doublet are the result of a coherent transfer of polarization. The cross peaks connecting the two doublets are due to spin diffusion. The differences of the intensities within each square of cross peaks are caused partly by the relatively strong dipolar coupling, partly by a slight missetting of the 90° pulse length.

The second mixing pulse will then convert polarization into observable coherence, which precesses under the same Hamiltonian as during the evolution period:

$$\sigma(t_1,\tau_m,t_2)=S_{1x}p_1\cos(\Omega_1 t_2)+S_{1y}p_1\sin(\Omega_1 t_2) +S_{2x}p_2\cos(\Omega_2 t_2)+S_{2y}p_2\sin(\Omega_2 t_2), \tag{96}$$

$$p_i=\tfrac{1}{2}[\cos(\Omega_i t_1)(1+e^{W_z^{(23)}\tau_m})+\cos(\Omega_k t_1)(1-e^{W_z^{(23)}\tau_m})], \quad i\neq k;\ i,k=1,2. \tag{97}$$

After Fourier transformation of the acquired signal, we find then the following diagonal (D) and cross-peak (C) amplitudes:

$$D=\tfrac{1}{2}(1+e^{W_z^{(23)}\tau_m}),\quad C=\tfrac{1}{2}(1-e^{W_z^{(23)}\tau_m}). \tag{98}$$

One example of a resulting spectrum is shown in Fig. 10.

To eliminate the effects of possibly non-negligible spin-lattice relaxation during the mixing period, we may calculate the ratio of cross-peak intensity to diagonal peak intensity which is independent of relaxation, provided both spins relax with equal rates,

$$\frac{C}{D}=\frac{1-e^{W_z^{(23)}\tau_m}}{1+e^{W_z^{(23)}\tau_m}}. \tag{99}$$

We may solve this equation for $W_z^{(23)}$:

$$W_z^{(23)}=\frac{1}{\tau_m}\ln\left[\frac{D-C}{D+C}\right]. \tag{100}$$

Experimentally it is useful, however, to repeat the measurement for different mixing times τ_m and to determine the spin-diffusion rate by a least-squares analysis of the experimental data. Experimental data from such a series of measurements are shown in Fig. 11.

C. Experimental results

Malonic acid, doubly ^{13}C labeled at the two carboxylic positions and embedded in a matrix of natural abundance molecules, represents an almost ideal system of two spins $S=\frac{1}{2}$ coupled to a large number of extraneous spins $I=\frac{1}{2}$. Since the doubly labeled molecules show a well-

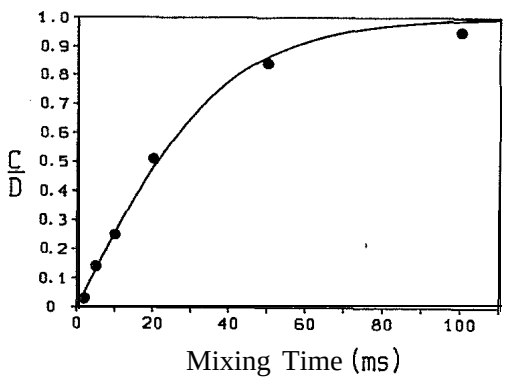

FIG. 11. Experimental determination of the spin-diffusion rate in a single crystal of malonic acid—$^{13}C_2$ (orientation 2). Six experimental points are shown together with a best exponential fit.

resolved dipolar coupling, this system makes it possible to check the validity of Eq. (36) for the calculation of the spin-diffusion rate.

In addition to measuring the spin-diffusion rate, the line shape of the zero-quantum transition had to be determined. This was done for two different orientations of the crystal with comparable dipolar couplings but different offsets and different linewidths. The spectra for the orientation with the smaller resonance offset (orientation 1) are shown in Fig. 12. The spin-diffusion rate was determined as described above. All parameters which occur in Eq. (36),

$$T_{SD}^{-1}=\frac{d^2}{(T_2^{ZQT})^{-2}+\delta^2}(T_2^{ZQT})^{-1},$$

can now be evaluated independently. The results for the two chosen orientations are as follows:

Orientation 1	Orientation 2
$\frac{1}{2\pi}d=230$ Hz	$\frac{1}{2\pi}d=250$ Hz
$\frac{1}{2\pi}\delta=1200$ Hz	$\frac{1}{2\pi}=3530$ Hz
$T_2^{ZQT}=137\ \mu s$	$T_2^{ZQT}=78.3\ \mu s$
$T_{SD}(calc)=7.2$ ms	$T_{SD}(calc)=20.8$ ms
$T_{SD}(expt)=6.7$ ms	$T_{SD}(expt)=19.15$ ms

These data show in both cases agreement between the experimental spin-diffusion time constant $T_{SD}(expt)$ and the spin-diffusion time constant $T_{SD}(calc)$ computed from zero-quantum linewidth, offset, and dipolar coupling constant according to Eq. (36).

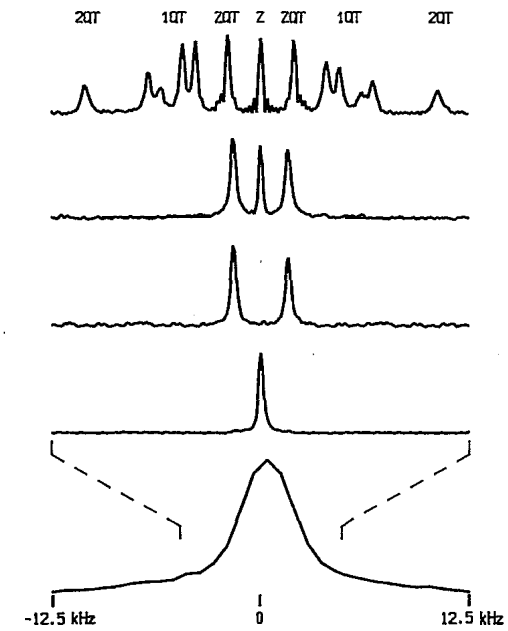

FIG. 12. Measurement of the line shape $g^{(23)}(\omega)$ of the zero-quantum transition in doubly ^{13}C-labeled malonic acid (orientation 1). In the top trace, the full proton-decoupled multiple-quantum spectrum is shown. The next trace shows the result of applying a four-step phase cycle in order to eliminate one- and two-quantum coherence. By the insertion of an additional free precession period also the center peak, due to longitudinal magnetization, could be eliminated (trace 3). The insertion of a 180° refocusing pulse shifts both zero-quantum lines to the center of the spectrum (trace 4). Except for the bottom trace, all are proton decoupled. The bottom trace shows the proton-coupled zero-quantum. line shape. Note the wider scale of this trace.

V. MEASUREMENTS OF ^{14}N SPIN DIFFUSION

In order to measure the dependence of the spin-diffusion rate on the difference in resonance frequency of two spins, it turned out to be useful to choose a quadrupolar system. ^{14}N resonance in ammonium sulfate was selected. Since the quadrupolar splitting [$\sim$200 kHz in $(NH_4)_2SO_4$] is usually much larger than all dipolar couplings, it is possible to vary the spectral distance of two resonance lines by slightly reorienting a single crystal without appreciably affecting dipolar couplings. Since the available rf fields were not sufficiently strong to cover the full spectral range of 200 kHz, only half of the spectrum was excited.

A. Evolution of the spin system

The same experimental method as in the case of the spin-$\frac{1}{2}$ system was used. The relevant Hamiltonian during evolution and detection is here

$$\mathcal{H}=q_1(S_{1z}^2-\tfrac{2}{3}\mathbb{1})+q_2(S_{2z}^2-\tfrac{2}{3}\mathbb{1}). \quad (101)$$

For equal sign of the two quadrupolar coupling constants, the initial condition created by the selective cross-polarization process is proportional to

$$\sigma(0)=S_{1x}^{(10)}+S_{2x}^{(10)}, \quad (102)$$

where the upper index indicates a single transition operator corresponding to the $m=1$ to m 0 transition. The density operator after the evolution period is

$$\sigma(t_1)=S_{1x}^{(10)}\cos(q_1t_1)+S_{1y}^{(10)}\sin(q_1t_1)+S_{2x}^{(10)}\cos(q_2t_1)+S_{2y}^{(10)}\sin(q_2t_1). \quad (103)$$

Th.e first $(\pi/2)_{-y}$ mixing pulse on the (1,0) transitions converts the x component into polarization. We neglect again coherence which decays during the mixing period and obtain for $\sigma(t_1,0)$,

$$\sigma(t_1,0)=S_{1z}^{(10)}\cos(q_1t_1)+S_{2z}^{(10)}\cos(q_2t_1)=\tfrac{1}{4}(S_{1z}+3S_{1z}^2-2)\cos(q_1t_1)+\tfrac{1}{4}(S_{2z}+3S_{2z}^2-2)\cos(q_2t_1). \quad (104)$$

The selective excitation therefore creates a mixture of Zeeman and quadrupolar order. By spin diffusion it evolves into [compare Eqs. (62)–(66)]

$$\sigma(t_1,\tau_m)=\tfrac{1}{8}\{S_{1z}[s+d\exp(-\tau_m/T_{SD}^{Z})]+S_{2z}[s-d\exp(-\tau_m/T_{SD}^{Z})]+(3S_{1z}^2-2)[s\exp(-\tau_m/T_{SD}^{Q\Sigma})+d\exp(-\tau_m/T_{SD}^{Q\Delta})]+(3S_{2z}^2-2)[s\exp(-\tau_m/T_{SD}^{Q\Sigma})-d\exp(-\tau_m/T_{SD}^{Q\Delta})]\}\ , \tag{105}$$

with

$$s=\cos(q_1t_1)+\cos(q_2t_1)\ ,\qquad d=\cos(q_1t_1)-\cos(q_2t_1)\ . \tag{106}$$

For equal sign of the coupling constants, $T_{SD}^{Q\Sigma}\simeq\infty$ and $T_{SD}^{Z}=3T_{SD}^{Q\Delta}$. The magnetization which is finally detected after the second mixing pulse leads then to the following relative peak intensities:

$$C=\tfrac{1}{8}[4-\exp(-\tau_m/3T_{SD}^{Q\Delta})-3\exp(-\tau_m/T_{SD}^{Q\Delta})]\ ,$$
$$D=\tfrac{1}{8}[4+\exp(-\tau_m/3T_{SD}^{Q\Delta})+3\exp(-\tau_m/T_{SD}^{Q\Delta})]\ . \tag{107}$$

Therefore, the time dependence of the ratio C/D is biexponential. As can be seen from Fig. 13, however, it is difficult to detect experimentally the slight deviation from a single exponential.

B. Experimental results

The spin-diffusion time was measured for two pairs of lines at five slightly different crystal orientations chosen so as to produce differences in quadrupolar splittings between 200 Hz and 2.5 kHz. The resulting dependence on the difference of resonance frequencies is shown in Fig. 14. The spin-diffusion times are within experimental error proportional to the square of the offset for both line pairs, indicating that the perturbation theory used to derive the expression for the spin-diffusion rate is applicable in this case.

These experimental results suggest possible applications of spin-diffusion measurements.[14,1,16,1] A measurement of the rate of spin diffusion between two spins provides information on the size of the respective dipolar coupling constant and on the distance between the two spins. In the case of ammonium sulfate this information allows one to assign the resonance lines to the two ^{14}N sites in the crystal which had not been possible previously.[33]

The dipolar coupling constant d can be deduced from the measured rate constants by means of Eqs. (46) and (66). The required zero-quantum linewidths could not be measured in this case, but a good estimate can be obtained from T_2^{1QT}, the relaxation time of single-quantum coherence as $T_2^{ZQT}=\frac{1}{2}T_2^{1QT}$, which holds if the two spins relax independently. The numerical values for the two pairs of nuclei are $d^a=1.5$ Hz and $d^b=5.7$ Hz. This may be compared with the values calculated from the crystal structure. Numerous dipolar couplings contribute to spin diffusion between two classes of spins and the effective spin-diffusion rate is determined by the average over the squares of the respective couplings for which the values 1.6 and 6.5 Hz were computed. The good agreement between the two data sets allows an unambiguous assignment of the line pairs to the nuclear positions.

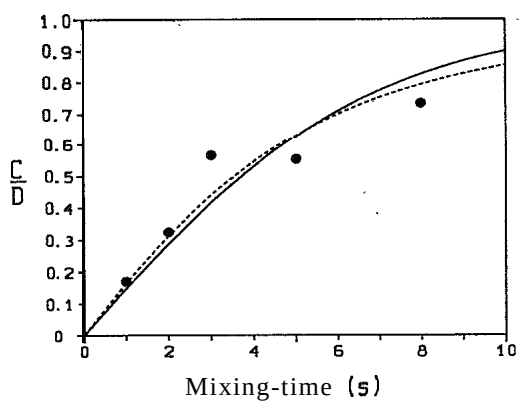

FIG. 13. Experimental determination of the ^{14}N spin-diffusion rate in an ammonium sulfate single crystal. The ratio of cross-peak intensity over diagonal peak intensity of Iine pair (a) has been measured for five different mixing times τ_m and an offset of 360 Hz. The experimental values do not allow one to discriminate between the expected nonexponential behavior (dashed curve) and the approximation by a single exponential (solid curve).

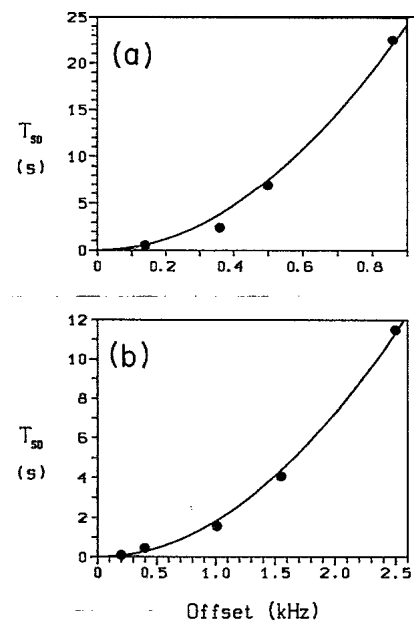

FIG. 14. ^{14}N spin-diffusion times $T_{SD}=T_{SD}^{Q\Delta}=\frac{1}{3}T_{SD}^{Z}$ in ammonium sulfate for the two nonequivalent sites as a function of the offset between the two resonance lines. The offset is varied by a slight reorientation of the crystal. The orientation of the crystal is such that the magnetic field is close to the crystallographic a axis. The Iine pair (a) has a quadrupole coupling constant of 60 kHz, the Iine pair (b), of 80 kHz. The experimental points are shown together with a best fit by a parabola.

VI. MEASUREMENT OF DEUTERIUM SPIN DIFFUSION

Deuterium resonance in fully deuterated malonic acid has features similar to ^{14}N resonance in ammonium sulfate. There is again the possibility of varying the spectral separation of the resonance lines by a slight reorientation of the crystal which is small enough to leave the dipolar couplings virtually invariant. In addition, it is possible to discriminate between single- and double-quantum spin diffusion by measuring the diffusion of Zeeman and quadrupolar order separately. Since this crystal contains only one spin species, the features associated with spin diffusion in homonuclear systems, discussed in Secs. II D and III C, may be investigated experimentally.

A. Evolution of the spin system

1. Observation of Zeeman order

The density operator after nonselective preparation is

$$\sigma(0)=S_{1x}+S_{2x}\,. \tag{108}$$

It evolves under the Hamiltonian of Eq. (101) to

$$\sigma(t_1)=S_{1x}\cos(q_1t_1)+(S_{1y}S_{1z}+S_{1z}S_{1y})\sin(q_1t_1) +S_{2x}\cos(q_2t_1)+(S_{2y}S_{2z}+S_{2z}S_{2y})\sin(q_2t_1)\,. \tag{109}$$

As before, a $(\pi/2)_{-y}$ mixing pulse is applied and only longitudinal terms are kept:

$$\sigma(t_1,0)=S_{1z}\cos(q_1t_1)+S_{2z}\cos(q_2t_1)\,. \tag{110}$$

Spin diffusion leads to

$$\sigma(t_1,\tau_m)=\tfrac{1}{2}\{S_{1z}[s+d\exp(-\tau_m/T_{SD}^Z)] +S_{2z}[s-d\exp(-\tau_m/T_{SD}^Z)]\}\,, \tag{111}$$

with s and d defined in Eq. (106). After the last $(\pi/2)_y$ pulse, the signal is acquired and Fourier transformed to yield the following peak intensities:

$$C=\tfrac{1}{2}[1-\exp(-\tau_m/T_{SD}^Z)]\,,\qquad D=\tfrac{1}{2}[1+\exp(-\tau_m/T_{SD}^Z)]\,. \tag{112}$$

Each spin gives rise to two lines on the diagonal $\omega_1=\omega_2$ and two lines on the diagonal $\omega_1=-\omega_2$, all of equal intensity. For a two-spin system we find eight diagonal peaks with the same intensity, as well as eight spin-diffusion cross peaks. A typical spectrum is shown in Fig. 15.

2. *Observation of quadrupolar order*

If the first mixing pulse is a $(\pi/4)_x$ pulse, then the density operator at the beginning of the mixing period becomes

$$\sigma(t_1,0)=S_{1x}\cos(q_1t_1)+(S_{1z}^2-S_{1y}^2)\sin(q_1t_1) +S_{2x}\cos(q_2t_1)+(S_{2z}^2-S_{2y}^2)\sin(q_2t_1)\,, \tag{113}$$

and after coherences have been eliminated,

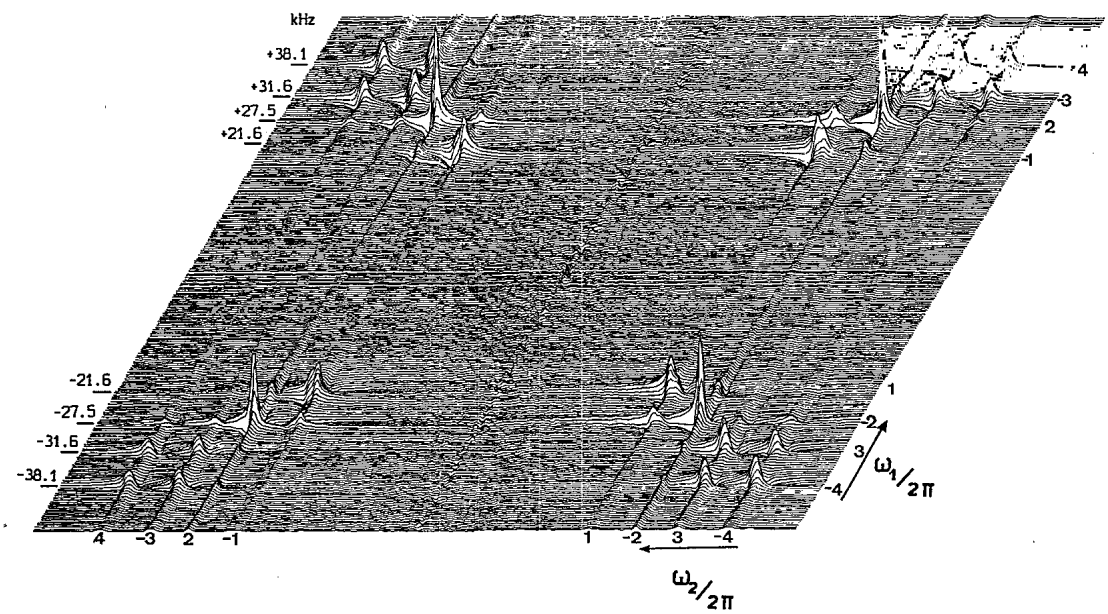

FIG. 15. Measurement of the diffusion of deuterium Zeeman order in malonic acid—d_4 (orientation 3), with B_0 parallel to the direction *(0.544, −0.734, 0.405) in* the standard orthogonal system. The lines on the main diagonal $\omega_1=\omega_2$ (lower right to upper left) correspond to the 1D spectrum of four nonequivalent deuterons with quadrupole coupling constants $q/2\pi$ of 21.6, 27.5, 31.6, and 38.1 kHz. The transitions labeled ±1, ±2 belong to the carboxylic deuterons, those labeled ±3, ±4 to the methylene deuterons. Negative coordinates mark $m=-1\rightarrow m=0$ transitions, positive coordinates mark $m=0\rightarrow m=1$ transitions. The lines at $\omega_1=-\omega_2$ are due to a coherent exchange of magnetization between the two transitions belonging to the same spin. The remaining lines are due to spin diffusion.

$$\sigma(t_1,0+)=(\tfrac{3}{2}S_{1z}^2-\mathbb{1})\sin(q_1t_1)+(\tfrac{3}{2}S_{2z}^2-\mathbb{1})\sin(q_2t_1)\ . \tag{114}$$

This pulse sequence therefore creates pure quadrupolar order. If the transmitter is not exactly on resonance, or if quadrature detection in ω_1 is used, some Zeeman order may be created in addition. It is possible to suppress the undesired Zeeman order by adding two experiments, in one of which the Zeeman order is inverted with a π pulse during the mixing period. Spin diffusion of pure quadrupolar order then leads after the mixing period to

$$\begin{aligned}\sigma(t_1,\tau_m)=&(\tfrac{3}{2}S_{1z}^2-1)\tfrac{1}{2}[s\exp(-\tau_m/T_{SD}^{Q\Sigma})\\ &+d\exp(-\tau_m/T_{SD}^{Q\Delta})]\\ +&(\tfrac{3}{2}S_{2z}^2-1)\tfrac{1}{2}[s\exp(-\tau_m/T_{SD}^{Q\Sigma})\\ &-d\exp(-\tau_m/T_{SD}^{Q\Delta})]\ ,\end{aligned} \tag{115}$$

where in contrast to Eq. (106)

$$\begin{aligned}s&=\sin(q_1t_1)+\sin(q_2t_1)\ ,\\ d&=\sin(q_1t_1)-\sin(q_2t_1)\ ,\end{aligned} \tag{116}$$

and the resulting peak intensities are

$$\begin{aligned}|C|&=\tfrac{1}{2}|[\exp(-\tau_m/T_{SD}^{Q\Sigma})-\exp(-\tau_m/T_{SD}^{Q\Delta})]|\ ,\\ |D|&=\tfrac{1}{2}[\exp(-\tau_m/T_{SD}^{Q\Sigma})+\exp(-\tau_m/T_{SD}^{Q\Delta})]\ .\end{aligned} \tag{117}$$

The peaks occur at the same positions as in the measurement of Zeeman order. However, the peaks on the diagonal $\omega_1=\omega_2$ are positive, while those on the diagonal $\omega_1=-\omega_2$ are negative. The cross-peak amplitudes have the same sign as the corresponding diagonal peaks.

B. Experimental results

Figures 16 and 17 show two pairs of spectra, comparing diffusion of Zeeman and quadrupolar order. Whereas in Fig. 16 both Zeeman order and quadrupolar order diffuse, in Fig. 17 only Zeeman order is transferred. Figure 16 therefore represents an example for single-quantum spin diffusion, while Fig. 17 suggests a double-quantum process. The absence of a single-quantum spin diffusion in this case, put into evidence by the missing diffusion of quadrupolar order, is not yet fully understood.

We also measured the offset dependence of the spin-diffusion times. The results for single-quantum spin diffusion are shown in Fig. 18, those for double-quantum spin diffusion in Fig. 19. The results indicate the predicted quadratic offset dependence in the case of single-quantum spin diffusion, while in the case of double-quantum spin diffusion, the offset dependence is much stronger; it is approximately proportional to the fourth power of the offset. This is consistent with the prediction reached in Sec. II C 3 that double-quantum spin-diffusion processes should only be observable when the S_1-S_2 dipolar coupling becomes so strong that the second-order perturbation treatment breaks down.

It is also interesting to compare the spin-diffusion times of Zeeman and quadrupolar order. A purely kinetic analysis [Eq. (66)] predicts that quadrupolar order should diffuse three times faster than Zeeman order. The ratio found experimentally for large offsets is only 2.2. The difference between these values can be attributed to the finite heat capacity of the dipolar bath. As is shown in Fig. 20, a numerical evaluation of the time evolution given by Eq. (89) gives a consistent result for a spin-diffusion time $T_{SD}^{Q\Delta}=\frac{1}{3}T_{SD}^{Z}$ and a dipolar relaxation time $T_{1D}=0.16$ s, which is of the expected order of magnitude in view of a spin-lattice relaxation time of 2 s.

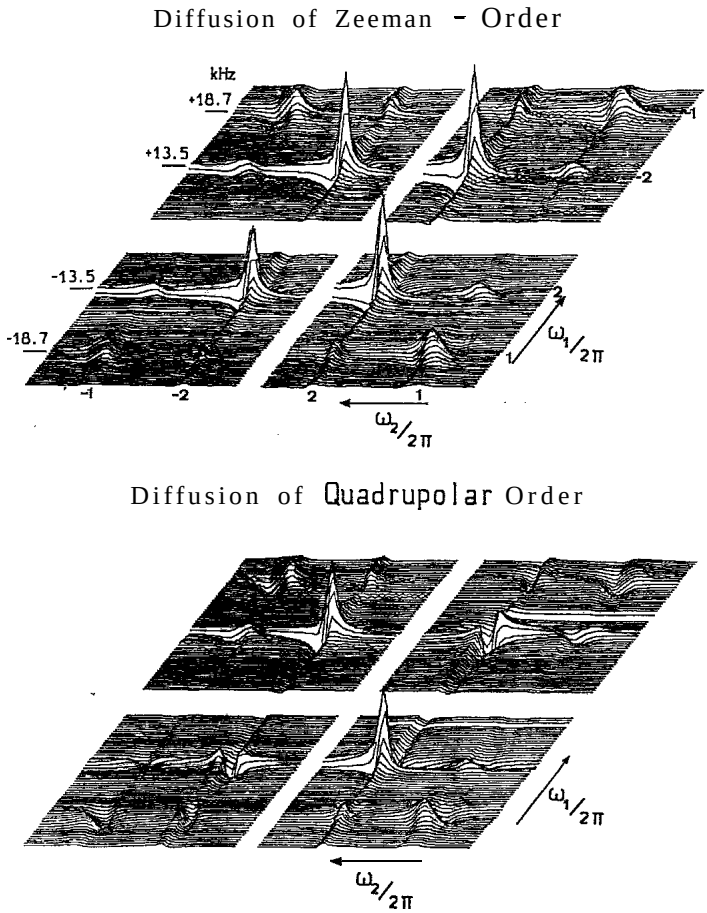

FIG. 16. Comparison of the diffusion of Zeeman order with the diffusion of quadrupolar order in malonic acid-d_4 for crystal orientation 4, with B_0 parallel to (0.467, -0.878, 0.098). In the upper half, a partial spectrum monitoring the exchange of Zeeman order is shown. The transitions are labeled with the same numbers as in Fig. 15. In the lower half, the same area of a 2D spectrum monitoring the diffusion of quadrupolar order is shown. The peaks on the diagonal $\omega_1=-\omega_2$ and the cross peaks in these quadrants [e.g., lines $(1,-1),(1,-2)$, etc.] are inverted in this case. The spin-diffusion cross peaks in the lower spectrum for $\tau_m=2$ s show about the same intensity as in the upper spectrum for a mixing time $\tau_m=6$ s, indicating clearly that quadrupole order is transferred faster than Zeeman order.

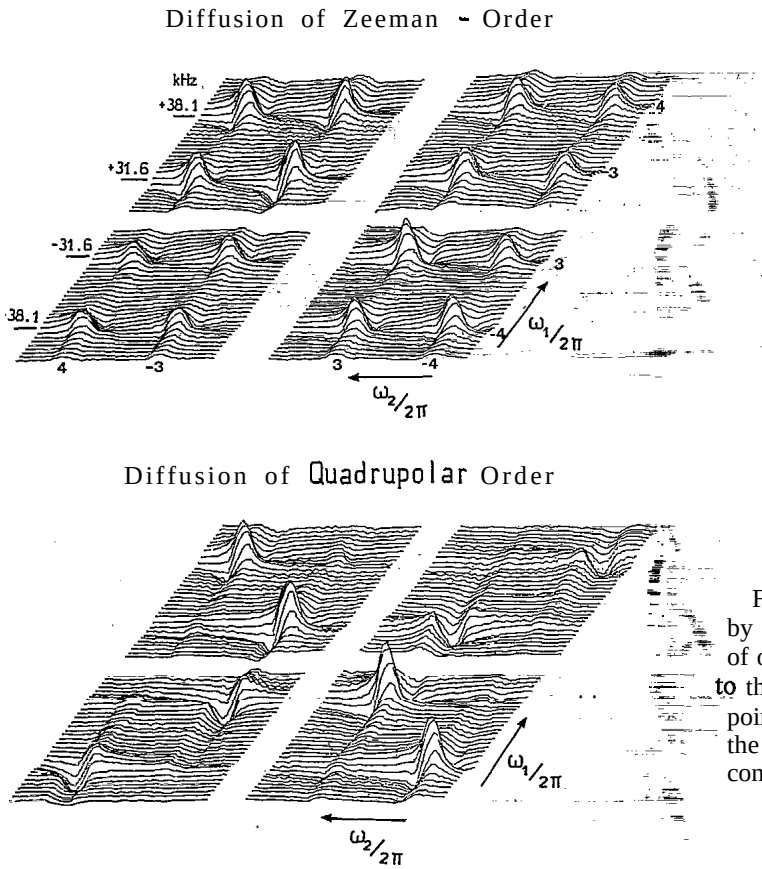

FIG. 17. Two-dimensional Zeeman and quadrupolar spin-diffusion spectra of malonic acid—d_4 for crystal orientation 3. The upper spectrum shows part of Fig. 15 and the transitions are labeled with the same numbers. The behavior is different from that in Fig. 16. In the upper **spectrum the lines which indicate spin diffusion such as (−3,−4),(3,4), etc., show almost the same intensity as the diagonal peaks, indicating that transfer of Zeeman order is virtually complete, while their absence in the** lower **spectrum indicates that no quadrupolar order is transferred.**

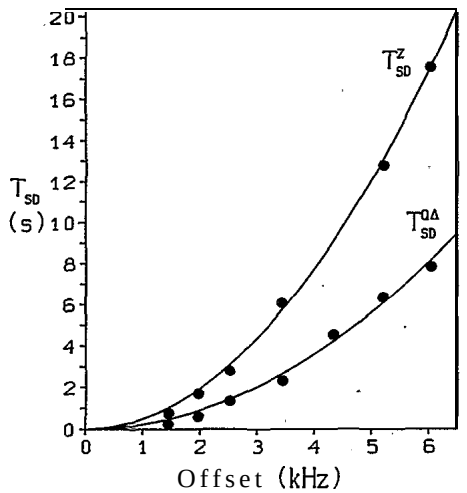

FIG. 18. Offset dependence of the ^{2}D spin-diffusion times T^Z_{SD} **and** T^{QA}_{SD} **in malonic acid—d_4 for the case of single-quantum spin diffusion (crystal orientation 4). Comparison of** T^Z_{SD} **with** T^{QA}_{SD} demonstrates again that the exchange of quadrupolar order is faster than that of Zeeman order. The curves represent best fits of the experimental data by parabolas.

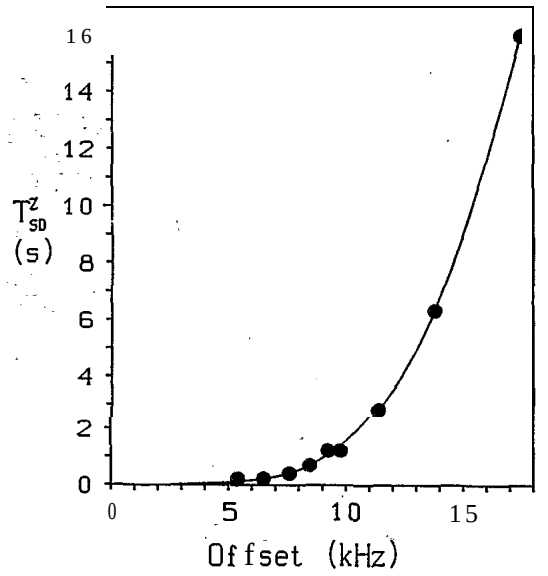

FIG. 19. Spin-diffusion times for diffusion of Zeeman order by double-quantum spin flips in malonic acid—d_4 as a function of offset for crystal orientation 3. The curve is shown as a guide to the eye and has no theoretical significance. The experimental points deviate strongly from the quadratic behavior found in all the previous cases. This can be explained by the violation of the conditions for the validity of the perturbation treatment.

VII. CONCLUSIONS

The agreement of experimental and theoretical results verifies that the calculation of the spin-diffusion rate in resolved spectra by perturbation theory is applicable to many practical situations. The spin-diffusion rate is proportional to the square of the dipolar coupling and to the amplitude of the zero-quantum spectrum evaluated at

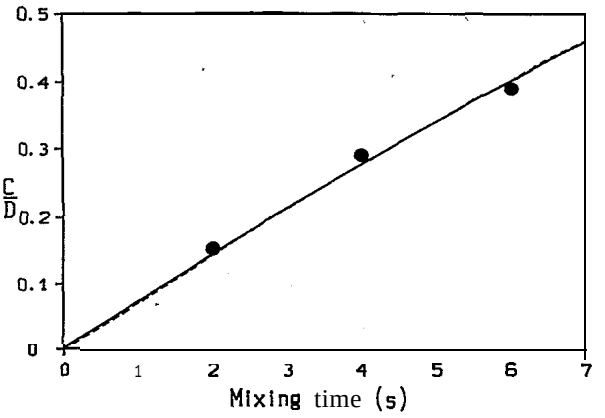

FIG. 20. **Ratio** of cross- to diagonal peak intensity' C/D **as a function of the mixing time** for diffusion of quadrupolar order in malonic acid—d_4 for an offset of $\delta/2\pi = 6.04$ kHz. **The experimental data** are compared with a numerical evaluation of Eq. (89) with the parameters $T^{QA}_{SD} = \frac{1}{3}T^Z_{SD} = 5.86$ **s, determined from the measurement of diffusion of Zeeman order,** $C_{SS} = 4.92$ kHz^2, **as estimated from the measured linewidths and** $T_{1D} = 0.16$ **s. The calculated behavior (solid line) almost coincides with a single exponential with a spin diffusion time** $T^{QA}_{SD} = 7.03$ s (dashed line).

$\omega=0$. For offsets larger than the linewidth, the spin-diffusion rate becomes inversely proportional to the square of the offset, except for cases when the perturbation treatment breaks down. The dominant spin-diffusion mechanism was found to be a single-quantum process, while double-quantum processes have also been detected in the case of very strong dipolar coupling. In the latter case, second-order perturbation theory becomes inapplicable and the offset dependence starts to deviate from the quadratic behavior. Single-quantum spin diffusion contributes to the diffusion of Zeeman as well as quadrupolar order, while the double-quantum mechanism causes exclusively the diffusion of Zeeman order.

The conservation of energy in the course of spin diffusion among nonequivalent spins is either established by the heteronuclear coupling to abundant extraneous spins with a strong homonuclear dipolar interaction or by the dipolar interaction among the involved spins themselves. In the latter case, the heat capacity of the dipolar reservoir is often too small to allow spin diffusion to proceed to completion. The bottleneck for spin diffusion is then the spin-lattice relaxation of the dipolar bath.

All experiments presented in this paper have been performed on 100% abundant spins. The theory presented here remains applicable even in dilute systems for the Calculation of spin diffusion between individual spins. However, it is no longer possible to assume that classes of "equivalent" spins remain internally in thermodynamic equilibrium because the rate constants depend on the random spatial separations of the dilute spins. Here, the rate of polarization exchange among equivalent spins becomes important, leading to a very complex network of rate processes and to nonexponential time dependence.

Single crystals were selected for all the measurements presented here to allow comparison with theory. However, practical applications of spin-diffusion measurements are envisaged mainly in disordered systems.[16,17] Spin diffusion may provide structural information on heterogeneous systems such as polymer blends, biological materials, and minerals.

In polycrystalline or amorphous systems, magic angle sample spinmng must normally be applied to obtain sufficient spectral resolution. Spin diffusion is strongly influenced by the sample spinning. For small angular velocity, spinning leads to an averaging of the spin-diffusion rate over the various microcrystallite orientations. It has been shown[9,34] that this may considerably enhance the spin-diffusion rate. For a rotation rate equal to a submultiple of the offset between two resonance lines, the rotation may even provide the energy balance which is required for the spin-diffusion process.[35] On the other hand, if the spuming rate exceeds the dipolar couplings, they are averaged to zero and spin diffusion is quenched.[36] We should mention that related problems of spin diffusion have also been investigated in other fields, such as electron spin resonance.[37-39]

ACKNOWLEDGMENTS

This research has been supported by the Swiss National Science Foundation. The authors are grateful to Guido Grassi for the synthesis of ^{13}C-labeled malonic acid and to Pablo Caravatti and Malcohn H. Levitt for helpful discussions.

[1] N. Bloembergen, Physica 15,386 (1949).
[2] S. R. Hartmann and E. L. Hahn, Phys. Rev. 128, 2042 (1962).
[3] A. Pines, M. G. Gibby, and J. S. Waugh, J. Chem. Phys. 59, 569 (1973).
[4] M. H. Levitt, D. Suter, and R. R. Ernst (unpublished).
[5] R. de L. Kronig and C. J. Bouwkamp, Physica 5,521 (1938).
[6] R. de L. Kronig and C. J. Bouwkamp, Physica 6,290 (1939).
[7] N. Bloembergen, S. Shapiro, P. S. Pershan, and J. 0. Artman, Phys. Rev. 114,445 (1959).
[8] A. C. Lind, J. Chem. Phys. 66, 3482 (1977).
[9] M. Alla, R. Eckman, and A. Pines, Chem. Phys. Lett. 71, 148 (1980).
[10] W. Schajor, N. Pislewski, H. Zimmermann, and U. Haeberlen, Chem. Phys. Lett. 76,409 (1980).
[11] C. Ye, R. Eckman, and A. Pines, J. Magn. Reson. 55, 334 (1983).
[12] D. C. Douglass and V. J. McBrierty, Macromolecules 11, 766 (1978).
[13] V. J. McBrierty, Faraday Discuss. Chem. Soc. 68, 78 (1979).
[14] P. Caravatti, J. A. Deli, G. Bodenhausen, and R. R. Ernst, J. Am. Chem. Soc. 104, 5506 (1982).
[15] N. M. Szevemyi, M. J. Sullivan, and G. E. Maciel, J. Magn. Reson. 47,462 (1982).
[16] P. M. Henrichs and M. Linder, J. Magn. Reson. 58, 458 (1984).
[17] P. Caravatti, P. Neuenschwander, and R. R. Ernst, Macromolecules 18, 119 (1985).
[18] W. E. Hull and B. D. Sykes, J. Chem. Phys. 63, 867 (1975).
[19] A. Kalk and H. J. C. Berendsen, J. Magn. Reson. 24, 343 (1976).
[20] S. L. Gordon and K. Wtithrich, J. Am. Chem. Soc. 101, 5152 (1979).
[21] Anil Kumar, R. R. Ernst, and K. Wtithrich, Biochem. Biophys. Res. Commun. 95, 1 (1980).
[22] Anil Kumar, G. Wagner, R. R. Ernst, and K. Wüthrich, J. Am. Chem. Soc. 103, 3654 (1981).
[23] D. Suter and R. R. Ernst, Phys. Rev. B 25, 6038 (1982).
[24] R. Eckman, A. Pines, R. Tycko, and D. P. Weitekamp, Chem. Phys. Lett. 99, 35 (1983).
[25] U. Haeberlen, 6th Spec. Coll. Ampere, Crete (1983) (unpublished).
[26] C. E. Bronniman, N. M. Szevemyi, and G. E. Maciel, J. Chem. Phys. 79, 3694 (1983).
[27] B. N. Provotorov, Zh. Eksp. Teor. Fiz. 41, 1582 (1961) [Sov. Phys.—JETP 14, 1126 (1962)].
[28] M. Goldman, *Spin Temperature and Nuclear Magnetic Reso-*

nance in Solids (Oxford University Press, Oxford, England, 1970), Chap. 4.
[29]A. Abragam, ***The Principles of Nuclear Magnetism*** (Oxford University Press, Oxford, England, 1961), Chap. 8.
[30]A. Wokaun and R. R. Ernst, J. Chem. Phys. 67, 1752 (1977).
[31]P. Borckmans and D. Walgraef, Phys. Rev. 167,282 (1968).
[32]J. Jeener, B. H. Meier, P. Bachmann, and R. R. Ernst, J. Chem. Phys. 71, 4546 (1979).
[33]R. Blinc, M. Mali, R. Osredkar, A. Prelesnik, J. Seliger, and I. Zupancic, Chem. Phys. Lett. 14, 49 (1972).
[34]R. Eckman, J. Chem. Phys. 79,524 (1983).
[35]E. R. Andrew, A. Bradbury, R. G. Eades, and V. T. Wynn, Phys. Lett. 4, 99 (1963).
[36]P. Caravatti (unpublished measurements, private communication).
[37]A. M. Portis, Phys. Rev. 104, 584 (1956).
[38]A. S. Epifanor and A. A. Manenkor, Zh. Eksp. Teor. Fiz. 60, 1804 (1971) [Sov. Phys.—JETP 33,976 (1971)].
[39]V. A. Atsarkin and M. I. Rodak, Usp. Fiz. Nauk 107, 3 (1972) [Sov. Phys.—Usp. 15, 251 (1972—1973)].